

# Time-Delay Observables for Koopman: Theory and Applications

Mason Kamb<sup>†</sup>, Eurika Kaiser<sup>\*</sup>, Steven L. Brunton<sup>\*</sup>, J. Nathan Kutz<sup>†</sup>

<sup>†</sup> Department of Applied Mathematics, University of Washington, Seattle, WA 98195, United States

<sup>\*</sup> Department of Mechanical Engineering, University of Washington, Seattle, WA 98195, United States

June 11, 2022

## Abstract

Nonlinear dynamical systems are ubiquitous in science and engineering, yet many issues still exist related to the analysis and prediction of these systems. Koopman theory circumvents these issues by transforming the finite-dimensional nonlinear dynamics to a linear dynamical system of functions in an infinite-dimensional Hilbert space of observables. The eigenfunctions of the Koopman operator evolve linearly in time and thus provide a natural coordinate system for simplifying the dynamical behaviors of the system. We consider a family of observable functions constructed by projecting the delay coordinates of the system onto the eigenvectors of the autocorrelation function, which can be regarded as continuous SVD basis vectors for time-delay observables. We observe that these functions are the most parsimonious basis of observables for a system with Koopman mode decomposition of order  $N$ , in the sense that the associated Koopman eigenfunctions are guaranteed to lie in the span of the first  $N$  of these coordinates. We conjecture and prove a number of theoretical results related to the quality of these approximations in the more general setting where the system has mixed spectra or the coordinates are otherwise insufficient to capture the full spectral information. We prove a related and very general result that the dynamics of the observables generated by projecting delay coordinates onto an arbitrary orthonormal basis are system-independent and depend only on the choice of basis, which gives a highly efficient way of computing representations of the Koopman operator in these coordinates. We show that this formalism provides a theoretical underpinning for the empirical results in [8], which found that chaotic dynamical systems can be approximately factored into intermittently forced linear systems when viewed in delay coordinates. Finally, we compute these time delay observables for a number of example dynamical systems and show that empirical results match our theory.

## 1 Introduction

Dynamical systems are ubiquitous in science and engineering. While linear systems are well-characterized, understanding nonlinear systems remains a open challenge. Nonlinear systems do not satisfy the linear superposition principle, can exhibit an extremely wide range of behaviors, including chaos, and do not generally admit analytic solutions. Koopman operator theory is an emerging framework for analyzing such systems. In this framework, the finite-dimensional nonlinear state space dynamics are transformed to an infinite-dimensional linear dynamical system in the Hilbert space of functions on the state, which is encoded in the Koopman operator [17, 18, 31]. The eigenfunctions of the Koopman operator provide a set of coordinates in which the dynamics of the system appear globally linear. While this framework is theoretically powerful, finding these eigenfunctions is a challenging problem which lacks principled approaches. The current leading algorithm for computing these eigenfunctions, the *dynamic mode decomposition* (DMD) [41, 38] and its extension to nonlinear observables, using either judiciously selected variables [22] or the *extended DMD* (EDMD) algorithm [51], require the a priori selection of a Koopman-invariant subspace in order to work effectively. If the observables are poorly selected, the resultant approximation to the Koopman operator and its eigenfunctions can be quite poor. In this work, we provide a general and computationally efficient approach to obtaining effective observable functions, which is based on a variant of delay

embedding.

Delay embedding is a classical approach to augmenting the information contained in the system state by augmenting it with measurements of the state history. Takens' seminal embedding theorem establishes that under certain technical conditions, delay embedding a signal coordinate of the system can reconstruct the attractor of the original system, up to a diffeomorphism [46]. Delay embedding methods have also been employed for system identification, most notably by the eigensystem realization algorithm (ERA) [14]. An additional variant to delay embedding was introduced by Broomhead and King in [4], which projects the delay embedded measurements onto the eigenvectors of the autocorrelation function. As these components tend to yield more information and are more robust to noise than generic embedding analysis, this technique has since been widely adopted in a variety of fields, notably as singular spectrum analysis (SSA) [49].

More recently, delay embedding has shown promise as a technique for computing Koopman eigenfunctions from data, both in regimes where only partial state information is available [8], as well as in regimes where full state information is available but more functions are needed to span a Koopman-invariant subspace [25]. Brunton et. al. [8] developed a variant of this technique, called the *Hankel Alternative View of Koopman* (HAVOK) analysis, which studied the linear dynamics of the projections of time-delay embedded systems onto the singular vectors of a Hankel matrix of the signal. They found the striking empirical result that even for systems where the assumption of Koopman-invariance does not hold, such as chaotic systems, the dynamics of these coordinates was nearly linear, and could be closed by including the action of a single, high-order forcing term. Mezic and Arbabi [1] later proved the convergence of these methods for ergodic systems under the assumption that the time-delay subspace was Koopman-invariant.

In the present work, we consider a generalization of HAVOK wherein the dynamics of the system are embedded in *convolutional coordinates*. These coordinates are given by the projections of time-delay coordinates onto a generic, infinite, orthonormal basis. We prove the striking result that the dynamics of these coordinates are linear and, for a given choice of basis, independent of the underlying system. The proof is straightforward, and to our knowledge has not been reported in the literature. Although this result is exact in the infinite-dimensional case, finite-dimensional truncations of these dynamics are generally poor at approximating the dynamics of the underlying system. We instead advocate for the use of the SVD basis of the Hankel matrix for the convolutional coordinates. We show that these coordinates have the following advantageous properties:

1. The analytically computed linear dynamics on the Hankel SVD basis match those estimated via a DMD-type algorithm.
2. For a nonlinear system that admits a Koopman mode expansion of order  $N$ , the dynamics of the first  $N$  convolutional coordinates exactly encode the dynamics of the system, and the associated Koopman eigenfunctions will be in the span of these coordinates. We know of no other family of observable functions that has a similar guarantee.
3. The Hankel SVD basis is also the basis of eigenvectors of the autocorrelation function of the signal. The intrinsic dynamical properties of these convolutional coordinates enable a dramatically faster DMD computation for this set of observables.

We prove and conjecture some results relating to the nature and quality of these approximations to the Koopman operator in a general setting. We compute the discrete approximations of these coordinates for a number of example systems and the associated Koopman spectrum and eigenfunctions. We observe that our methods generally work well and provide superior or comparable Koopman approximations to other families of observables. A few pathological cases are identified for which our method does not perform as expected. In these cases, the eigenvalues of the system are nearly degenerate and the delay embedding window is small.

## 2 Background

### 2.1 Koopman Theory

We consider an autonomous dynamical system on  $\mathbb{R}^n$  of the form

$$\frac{d}{dt}\mathbf{x}(t) = \mathbf{f}(\mathbf{x}(t)) \quad (1)$$

where  $\mathbf{x} \in \mathbb{R}^n$  represents the state of the system and  $\mathbf{f} : \mathbb{R}^N \rightarrow \mathbb{R}^n$  is a possibly nonlinear vector field. Here,  $t$  denotes time. For all applications in this paper, we will assume that  $\mathbf{f}$  is at least  $\mathcal{C}^1$  so that the trajectories  $\mathbf{x}(t)$  are at least  $\mathcal{C}^2$ . The system (1) induces a *flow map*  $\mathbf{F}_t$ , specifically a time-dependent family of maps  $\{\mathbf{F}_t\}_{t \in \mathbb{R}_+}$ , satisfying

$$\mathbf{x}(t) = \mathbf{F}_t(\mathbf{x}_0), \quad (2)$$

which yields the state  $\mathbf{x}(t)$  at time  $t$  given an initial state  $\mathbf{x}_0 := \mathbf{x}(0)$ .

B. O. Koopman and J. v. Neumann introduced an influential operator-theoretic perspective on dynamical systems of the above form [17, 18]. Their fundamental insight was that the finite-dimensional nonlinear dynamics of (1) can be transformed to an infinite-dimensional, linear dynamical system by considering the Hilbert space of scalar observable functions  $g : \mathbb{R}^N \rightarrow \mathbb{C}$  on the state, instead of the state directly. The one-parameter semigroup of *Koopman Operators*,  $\{\mathcal{K}_t\}_{t \in \mathbb{R}_+}$ , acting on observables  $g$  is defined by

$$\mathcal{K}_t g = g \circ \mathbf{F}_t, \quad (3)$$

where  $\circ$  denotes the composition operator so that

$$\mathcal{K}_t g(\mathbf{x}_0) = g(\mathbf{F}_t(\mathbf{x}_0)) = g(\mathbf{x}(t)). \quad (4)$$

$\mathcal{K}_t$  maps the measurement function  $g$  to the values it will take after the dynamics have progressed for a time  $t$ . The generator of the family of Koopman operators is defined as the following limit by

$$\mathcal{A}g = \lim_{t \rightarrow 0^+} \frac{1}{t} (\mathcal{K}_t g - g) = \frac{d}{dt} g, \quad (5)$$

assuming  $\mathbf{f}$  is smooth and globally Lipschitz [24, 30].

These operators are linear by construction and reflect the dynamics of the system in the space of observable functions. This framework allows us to transform the possibly complex, nonlinear dynamics in the finite-dimensional state space for infinite-dimensional linear dynamics in the space of observable functions on the state.

While this framework is theoretically appealing, it is difficult to work directly with the infinite-dimensional dynamics of (3). An alternative approach is to perform a spectral decomposition of the Koopman Operator [31]. This approach seeks the eigenvalues  $\lambda \in \mathbb{C}$  and eigenfunctions  $\varphi : \mathbb{R}^N \rightarrow \mathbb{C}$  of the Koopman operator, satisfying:

$$\mathcal{K}_t \varphi(\mathbf{x}_0) = \varphi(\mathbf{F}_t(\mathbf{x}_0)) = \varphi(\mathbf{x}_0) e^{\lambda t}. \quad (6)$$

Each eigenfunction can be considered as a special type of observable, which behaves linearly in time. Thus, the eigenspace of each eigenfunction  $\varphi$  is Koopman invariant by construction, so these functions provide coordinates in which the Koopman operator is naturally finite-dimensional.

Another use of the Koopman eigenfunctions is as a basis for the space of observables. If the Koopman operator family  $\mathcal{K}_t$  has a discrete spectrum consisting only of isolated eigenvalues, we can expand the dynamics of any vector-valued observable function  $\mathbf{g} : \mathbb{R}^n \rightarrow \mathbb{C}^d$  in a basis of these eigenfunctions:

$$\mathbf{g}(\mathbf{x}(t)) = \mathcal{K}_t \mathbf{g}(\mathbf{x}_0) = \sum_{j=0}^{\infty} \mathbf{c}_j \varphi_j(\mathbf{x}_0) e^{\lambda_j t}, \quad (7)$$

where  $\mathbf{c}_j$  is associated with the pair  $(\varphi_j, \lambda_j)$  and obtained by projecting the observable  $\mathbf{g}$  onto the Koopman eigenfunction  $\varphi_j$ . This decomposition is known as the *Koopman mode decomposition* [31]. This decomposition illustrates a powerful application of Koopman eigenfunctions. If a complete basis of these eigenfunctions exists, then the dynamics of any set of observables can be solved exactly and linearly using the expansion above.

The discrete-time dynamical system

$$\mathbf{x}_{n+1} = \mathbf{F}(\mathbf{x}_n), \quad (8)$$

may be obtained from a discretization of (1) with  $\mathbf{x}_n := \mathbf{x}(t_n)$ ,  $\Delta t := t_{n+1} - t_n$  and flow map  $\mathbf{F}$ . In discrete time, we have

$$\mathcal{K}\varphi(\mathbf{x}) = \varphi(\mathbf{F}(\mathbf{x})) = \lambda\varphi(\mathbf{x}), \quad (9)$$

where  $\mathcal{K}$  denotes here the Koopman operator.

$$\mathbf{g}(\mathbf{x}_n) = \mathcal{K}_{\Delta t}^n \mathbf{g}(\mathbf{x}_0) = \sum_{j=0}^{\infty} \mathbf{c}_j \varphi_j(\mathbf{x}_0) \lambda_j^n. \quad (10)$$

## 2.2 Dynamic Mode Decomposition

While the Koopman operator-theoretic perspective on dynamical systems dates back to the 1930s, it has only been in recent years that these methods have gained widespread attention. One reason for this is the variety of computational tools and algorithms that have been developed to aid the study of the Koopman operator and its spectral properties [31, 32, 9, 23, 33, 30]. One such class of methods is known as dynamic mode decomposition (DMD) [39, 38, 48, 21]. DMD was originally introduced in the fluid dynamics community as a tool for extracting spatiotemporal coherent structures from complex flows [40, 39]. It was later shown that the spatiotemporal modes obtained by DMD converge to the Koopman modes for a set of linear observables [38, 48]. This property of the DMD has made it one of the primary computational tools in Koopman Theory.

The exact DMD algorithm works as follows [48]. A snapshot matrix of state measurements  $\mathbf{X}$  is assembled. The algorithm estimates a linear relationship between the data matrices

$$\mathbf{X}_1 = \begin{pmatrix} | & | & & | \\ \mathbf{x}_1 & \mathbf{x}_2 & \cdots & \mathbf{x}_{M-1} \\ | & | & & | \end{pmatrix} \quad \mathbf{X}_2 = \begin{pmatrix} | & | & & | \\ \mathbf{x}_2 & \mathbf{x}_3 & \cdots & \mathbf{x}_M \\ | & | & & | \end{pmatrix}.$$

where  $\mathbf{x}_j = \mathbf{x}(t_j)$  denotes the  $j$ th timestep at discrete time  $t_j$  and  $\Delta t = t_{j+1} - t_j$  is the timestep between snapshots. The algorithm estimates the propagator matrix  $\mathbf{K} \in \mathbb{R}^{n \times n}$  that satisfies

$$\mathbf{X}_2 \approx \mathbf{K} \mathbf{X}_1 \quad (11)$$

The optimal  $\mathbf{K}$  is found by solving the optimization problem

$$\mathbf{K} = \arg \min_{\hat{\mathbf{K}}} \|\hat{\mathbf{K}} \mathbf{X}_1 - \mathbf{X}_2\|_F \quad (12)$$

where  $\|\cdot\|_F$  denotes the Frobenius norm defined as  $\|\mathbf{X}\|_F = \sqrt{\sum_{j=1}^N \sum_{k=1}^M X_{jk}^2}$ . The least-squares solution to this optimization problem is known to be  $\mathbf{K} = \mathbf{X}_2 \mathbf{X}_1^\dagger$  where  $\dagger$  denotes the Moore-Penrose pseudoinverse. Once an estimate for  $\mathbf{K}$  has been produced through this procedure, we can compute the eigendecomposition of  $\mathbf{K}$ :

$$\mathbf{K} = \mathbf{\Phi} \mathbf{\Lambda} \mathbf{\Phi}^{-1}. \quad (13)$$

The columns  $\phi_j \in \mathbb{R}^N$  of  $\mathbf{\Phi}$  are called the DMD *modes* of  $\mathbf{K}$ . While this optimization problem is typically solved using a naive least-squares solution, there exist alternative algorithms which produce a less biased set of DMD modes and eigenvalues. For details, see Askham and Kutz [2] for a comparison of existing techniques.

Using this eigendecomposition, we can predict the future solution approximately in the following form:

$$\mathbf{x}_n \approx \sum_{j=1}^N b_j \phi_j \lambda_j^n \quad (14)$$

where  $b_j$ 's are the coordinates of the initial state  $\mathbf{x}_1$  in the Koopman mode basis so that  $\mathbf{x}_1 = \Phi \mathbf{b}$ , i.e. initial amplitude of each mode  $\phi_j$ . In continuous-time, we obtain:

$$\mathbf{x}(t) \approx \sum_{j=1}^N b_j \phi_j e^{\omega_j t} \quad (15)$$

with the continuous-time eigenvalue  $\omega_j = \ln(\lambda_j)/\Delta t$ . Here,  $\phi_j$  and  $\lambda_j$  are the  $j$ th eigenvector-eigenvalue pair of  $\mathbf{K}$ .

In practice, this eigendecomposition may be prohibitively expensive to compute if the dimension of  $\mathbf{K}$  is large. This issue can be circumvented by computing the *singular value decomposition* (SVD) of  $\mathbf{X}_1 = \mathbf{U} \mathbf{\Sigma} \mathbf{V}^*$  and computing the  $r \times r$  truncated matrix  $\tilde{\mathbf{K}}$ :

$$\tilde{\mathbf{K}} = \mathbf{U}_r \mathbf{K} \mathbf{U}_r^* \quad (16)$$

where  $\mathbf{U}_r$  consists of the first  $r$  columns of  $\mathbf{U}$ . We then compute the eigendecomposition of  $\tilde{\mathbf{K}}$

$$\tilde{\mathbf{K}} = \tilde{\Phi} \tilde{\Lambda} \tilde{\Phi}^{-1}. \quad (17)$$

The full-state eigenvector matrix  $\Phi$  can then be estimated as follows:

$$\Phi = \mathbf{X}_2 \mathbf{V} \mathbf{\Sigma}^{-1} \tilde{\Phi}. \quad (18)$$

Related DMD algorithms and innovations include the optimized DMD [2], Bayesian DMD [43], and subspace DMD [44]. Optimized DMD exhibits particularly stable numerical properties [2].

In many real-world systems, the underlying system dynamics will not be linear, and thus the linear operator  $\mathbf{K}$  estimated by DMD will not provide a good approximation to the nonlinear system dynamics. We may instead decide to work with an augmented state consisting of possibly nonlinear functions of the state  $\mathbf{g} = (g_1, \dots, g_D)$ , where  $D$  is generally larger than the dimension of the original state  $N$ . We can then compute the DMD on the new data matrices

$$\mathbf{g}(\mathbf{X}_1) = \begin{pmatrix} | & | & & | \\ \mathbf{g}(\mathbf{x}_1) & \mathbf{g}(\mathbf{x}_2) & \cdots & \mathbf{g}(\mathbf{x}_{M-1}) \\ | & | & & | \end{pmatrix} \quad \mathbf{g}(\mathbf{X}_2) = \begin{pmatrix} | & | & & | \\ \mathbf{g}(\mathbf{x}_2) & \mathbf{g}(\mathbf{x}_3) & \cdots & \mathbf{g}(\mathbf{x}_M) \\ | & | & & | \end{pmatrix}.$$

This allows us to estimate a nonlinear model of the form  $\mathbf{g}^{-1} \circ \mathbf{K} \circ \mathbf{g}$  on the state  $\mathbf{x}$ . This procedure is known as the *extended dynamic mode decomposition* (EDMD) [51] or the variational approach of conformation dynamics (VAC) [34, 35]. The classic DMD is a special case of EDMD in the case where the measurement consists of the identity  $\mathbf{g}(\mathbf{x}) = \mathbf{x}$ .

A theoretical benefit of EDMD is that the estimated linear operators are known to converge to an orthogonal projection of the Koopman operator onto the subspace of observables spanned by  $\mathbf{g}$  in the limit of infinite data [19]. Furthermore, in the limit as the observables in  $\mathbf{g}$  span the Hilbert space of observable functions, the action of the Koopman operator can be exactly reconstructed [19]. However, EDMD is limited by the quality of the selection of observable functions, since a generic selection of a finite number of observables  $\mathbf{g}$  will not span a Koopman-invariant subspace [6] and thus the orthogonal projection may discard the relevant dynamics of the system. Augmenting  $\mathbf{g}$  with additional measurements increases the span of these observables and thus may result in a higher-quality approximation. However, this can result in an exceptionally large state, making EDMD prone to overfitting. The VAC approach explicitly cross-validates the resulting model to avoid overfitting [34, 35]. In some cases, machine learning methods [26] or domain knowledge [22] can result in a more effective observable selection. For example, Neural networks and deep learning have recently been used to great advantage to represent the Koopman operator [45, 52, 50, 29, 28, 36]. However, these techniques often lack formal justification.

## 2.3 Time Delay Embedding

A classic technique for dealing with partial state information is *delay embedding*. This method augments a state represented by a single (or few) measurement function with its past history, resulting in a new observable  $\tilde{\mathbf{g}}(\mathbf{x}(t)) =: (g(\mathbf{x}(t)), g(\mathbf{x}(t-\Delta t)), g(\mathbf{x}(t-2\Delta t)), \dots, g(\mathbf{x}(t-n\Delta t)), \dots, g(\mathbf{x}(t-(N-1)\Delta t))) \in \mathbb{R}^N$  with the lag time  $\Delta t$ . This is known as a *delay embedding* of the trajectory  $g(\mathbf{x}(t))$ . It was shown by Takens [46] that under mild conditions on the observable  $g$ , the dynamics of the delay vector  $\mathbf{y}$  are guaranteed to be diffeomorphic to the dynamics of the original state  $\mathbf{x}$ , provided that the embedding dimension is  $N \geq 2n + 1$ , where  $n$  is the dimension of the state. In many cases, a smaller embedding dimension may be chosen without sacrificing the diffeomorphism.

In practice, the quality of the reconstruction may depend greatly on parameter choices, such as the lag time  $\delta$  and the embedding dimension  $N$  [27, 13]. One approach for dealing with these issues is to compute the principal components of the trajectory [4, 49]. These are obtained by computing the SVD of a Hankel matrix on the trajectory data:

$$\mathbf{H} = \begin{pmatrix} g(\mathbf{x}_1) & g(\mathbf{x}_2) & \cdots & g(\mathbf{x}_M) \\ g(\mathbf{x}_2) & g(\mathbf{x}_3) & \cdots & g(\mathbf{x}_{M+1}) \\ \vdots & \vdots & \ddots & \vdots \\ g(\mathbf{x}_N) & g(\mathbf{x}_{N+1}) & \cdots & g(\mathbf{x}_{N+M-1}) \end{pmatrix} = \begin{pmatrix} \tilde{\mathbf{g}}(\mathbf{x}_1) & \tilde{\mathbf{g}}(\mathbf{x}_2) & \cdots & \tilde{\mathbf{g}}(\mathbf{x}_M) \\ \vdots & \vdots & \ddots & \vdots \\ \tilde{\mathbf{g}}(\mathbf{x}_N) & \tilde{\mathbf{g}}(\mathbf{x}_{N+1}) & \cdots & \tilde{\mathbf{g}}(\mathbf{x}_{N+M-1}) \end{pmatrix} = \mathbf{U}\Sigma\mathbf{V}^*.$$

The principal components (i.e. the right singular vectors of the SVD decomposition) of the trajectory are the columns of  $\mathbf{V}$ . Each row  $\mathbf{v}_j$  are the embeddings of the original states  $\mathbf{x}(t)$ . An appropriate dimension for the embedded state can be chosen by examining the singular value of each component and truncating after these pass below an appropriate threshold. Gavish and Donoho, for instance, provide a principled way to apply such thresholding [11].

This approach is advantageous because each principal component  $\mathbf{v}_j$  is normalized and uncorrelated with the other components of the trajectory. These ensure that the reconstructed attractor will not be *stretched* along a particular axis, and that each component carries as little redundancy with the others as possible. Furthermore, the subspace spanned by the first  $r$  principal components is the best rank- $r$  approximation of the trajectory space in a least-squares sense, so the principal component basis is in this sense an optimal basis for state-space reconstruction. We will return to these considerations at a later point.

The Hankel/delay embedded representation of the state trajectory has been recently connected to Koopman theory [8]. The Hankel matrix can be rewritten using the action of the Koopman operator on  $g$ :

$$\mathbf{H} = \begin{pmatrix} g(\mathbf{x}_1) & \mathcal{K}_{\Delta t}g(\mathbf{x}_1) & \cdots & \mathcal{K}_{\Delta t}^{M-1}g(\mathbf{x}_1) \\ \mathcal{K}_{\Delta t}g(\mathbf{x}_1) & \mathcal{K}_{\Delta t}^2g(\mathbf{x}_1) & \cdots & \mathcal{K}_{\Delta t}^Mg(\mathbf{x}_1) \\ \vdots & \vdots & \ddots & \vdots \\ \mathcal{K}_{\Delta t}^{N-1}g(\mathbf{x}_1) & \mathcal{K}_{\Delta t}^Ng(\mathbf{x}_1) & \cdots & \mathcal{K}_{\Delta t}^{M+N-2}g(\mathbf{x}_1) \end{pmatrix} = \begin{pmatrix} \tilde{\mathbf{g}}(\mathbf{x}_1) & \mathcal{K}_{\Delta t}\tilde{\mathbf{g}}(\mathbf{x}_1) & \cdots & \mathcal{K}_{\Delta t}^{M-1}\tilde{\mathbf{g}}(\mathbf{x}_1) \\ \vdots & \vdots & \ddots & \vdots \\ \tilde{\mathbf{g}}(\mathbf{x}_N) & \mathcal{K}_{\Delta t}\tilde{\mathbf{g}}(\mathbf{x}_N) & \cdots & \mathcal{K}_{\Delta t}^{M+N-2}\tilde{\mathbf{g}}(\mathbf{x}_N) \end{pmatrix}. \quad (19)$$

The delay-embedded state vector can be viewed as the vector of observables,  $\tilde{\mathbf{g}} = (g, \mathcal{K}_{\Delta t}g, \mathcal{K}_{\Delta t}^2g, \dots, \mathcal{K}_{\Delta t}^N g)$ . Due to the special connection with time delay observables and the Koopman operator, they are a natural basis for DMD and related Koopman spectral techniques. Delay embeddings have been used previously in DMD analyses in cases where only partial state information is available [5, 48]. Performing DMD on delay coordinates for linear systems is closely related to the eigensystem realization algorithm (ERA) [14] and singular spectrum analysis (SSA) [49]. A nonlinear variant of SSA based on Laplacian spectral analysis has been useful for time series with intermittent phenomena [12].

Brunton et. al. formally introduced this approach of performing a sparsified linear and nonlinear model regression on delay coordinates [7] and established the connection with Koopman theory and chaotic systems in [8]; the approach is referred to as the Hankel Alternative View of Koopman (HAVOK) analysis. They found that these coordinates provided nearly Koopman-invariant subspaces, as well as exhibiting several other interesting properties. Arbabi and Mezic later studied the properties of HAVOK models [1]. They establish that for ergodic systems, HAVOK converges to the true Koopman eigenfunctions and eigenvalues of the system. This convergence result is unusual for generic families of measurement functions, and

motivates the application of Koopman spectral methods to delay coordinates for systems where incomplete measurement data is available. Das and Giannakis have also investigated the spectrum of the Koopman operator in delay coordinates [10]. HAVOK models are also closely related to the Prony approximation of the Koopman decomposition [42].

Delay embedding can also be used to augment the state vector even when complete measurement data is available. This may be desirable for nonlinear systems with broad-spectrum behavior. The DMD can extract at most  $N$  dynamic modes and eigenvalues, where  $N$  is the dimension of vector  $\mathbf{y}$ . This is often insufficient for nonlinear systems, wherein a larger range of frequencies can be active even for a simple state. Le Clainche and Vega introduced *higher order dynamic mode decomposition* (HODMD) to circumvent these issues [25]. HODMD computes DMD on a state where the delay embedding is across multiple dimensions. The resultant state has dimension  $nN$ , where  $N$  is the length of the delay embedding and  $n$  is the dimension of the underlying state. They found that this approach was able to find a larger range of frequencies and produce more accurate reconstructions of the dynamics for a large variety of nonlinear systems.

### 3 Convolutional Coordinates

A common idea in signal processing is to extract features from signals by convolving with a filter function. For example, convolving signals with Gaussians is known to remove noise from the signal, while convolving the signal with a wavelet basis can be used to extract interpretable feature set for use in classification. Indeed, signal processing analysis is dominated by filtering of time series data. The fundamental insight of these approaches is that looking at local segments of the trajectory or signal offers more information than looking only at a single point. In addition to this, convolutions can also be thought of as linear coordinates on the time-delay embedded state of the trajectory. In this section, we develop a formalism for interpreting these coordinates as functions directly on the state space, which we call *convolutional coordinates*. While previous work on delay embedding coordinates has focused primarily on using delays and convolutions to extract/reconstruct *qualitative* information, we show that these convolutional coordinates also provide *quantitative* information about the system. We prove that in these coordinates, the dynamics of the system are intrinsically linear. Furthermore, the representation of these dynamics depends only on the choice of convolution functions, and not on the intrinsic dynamics of the system. We connect these results to Koopman theory and argue that these coordinates provide *system-independent representations* of the Koopman operator. These representations are intrinsically infinite-dimensional, and in general the maps obtained by projecting orthogonally onto do not coincide with the closest approximation of the Koopman on these coordinates. This makes these results interesting but not always suitable for practical usage. To circumvent this problem, careful attention must be paid to choose a basis for which these two maps coincide. One basis for which this holds are the eigenvectors of the autocorrelation function, which are discussed in section 4.

We consider the dynamical system defined in (1) with  $\mathbf{x} \in \mathbb{R}^n$  and an observable on this state  $\mathbf{g} : \mathbb{R}^n \rightarrow \mathbb{R}^k$ . In most applications of delay embedding, this observable is in fact a scalar (i.e.  $k = 1$ ), and  $\mathbf{g}(\mathbf{x})$  will select a single component of the state vector, e.g.  $\mathbf{g}(\mathbf{x}) = x_1$ .

Let  $\phi_j : [-\tau, \tau] \rightarrow \mathbb{R}^k$  be a differentiable, orthonormal basis on the interval  $[-\tau, \tau]$ , i.e. the inner product is  $\langle \phi_j, \phi_k \rangle := \int_{-\tau}^{\tau} \phi_j^T(s) \phi_k(s) ds = \delta_{jk}$  where  $\delta_{jk}$  is the Kronecker delta.

The value of the observable at time  $t + s$  is given by

$$\mathbf{g}(\mathbf{x}(t + s)) = \mathcal{K}_s \mathbf{g}(\mathbf{x}(t)) = \sum_{j=0}^{\infty} \mathbf{c}_j \varphi_j(\mathbf{x}(t)) e^{\lambda_j s} = \sum_{j=0}^{\infty} \mathbf{c}_j \varphi_j(\mathbf{x}_0) e^{\lambda_j t} e^{\lambda_j s}. \quad (20)$$

$$\mathbf{g}(\mathbf{x}(t + s)) = \sum_{j=0}^{\infty} w_j(\mathbf{x}(t)) \phi_j(s) \quad \forall s \quad (21)$$

We define the *convolutional coordinates*  $w_j$  as follows:

$$w_j(\mathbf{x}(t)) = \langle \phi_j, \mathbf{g}(\mathbf{x}(t + s)) \rangle = \int_{-\tau}^{\tau} \phi_j(s)^T \mathbf{g}(\mathbf{x}(t + s)) ds, \quad (22)$$

which can be written in terms of the Koopman operator  $\mathcal{K}_s$  as

$$w_j(\mathbf{x}(t)) = \int_{-\tau}^{\tau} \boldsymbol{\phi}_j(s) \mathcal{K}_s \mathbf{g}(\mathbf{x}(t)) ds. \quad (23)$$

Intuitively, these coordinates correspond to convolving the basis functions  $\boldsymbol{\phi}_j$  with the trajectory  $\mathbf{g}(\mathbf{x}(t))$  over the time window  $[-\tau, \tau]$ . Since the functions  $\boldsymbol{\phi}_j$  are orthonormal, the convolutional coordinates can also be thought of as the projections of these basis functions onto local segments of the trajectory  $\mathbf{g}(t + t')$  with  $t' \in [-\tau, \tau]$ . This suggests a connection between the coordinates  $w_j$  and the derivatives of  $\mathbf{g}$ . Even if observable  $g$  is an incomplete measurement of the underlying state  $\mathbf{x}$ , its future trajectory can in principle be reconstructed by computing its derivatives and expanding a Taylor series for later times. One consequence of this is that the dynamics of  $w_j$  appear linear. Furthermore, we can expand them analytically, as described in the following theorem.

**Lemma 1.** *The time derivative of an observable  $\mathbf{g}$  can be taken with respect to the basis functions  $\boldsymbol{\phi}(s)$  or coefficients  $w_j(\mathbf{x}(t))$ :*

$$\frac{d}{dt} \mathbf{g}(\mathbf{x}(t + s)) = \frac{d}{dt} \sum_{j=0}^{\infty} w_j(\mathbf{x}(t)) \boldsymbol{\phi}_j(s) = \sum_{j=0}^{\infty} \left( \frac{d}{dt} w_j(\mathbf{x}(t)) \right) \boldsymbol{\phi}_j(s) = \sum_{j=0}^{\infty} w_j(\mathbf{x}(t)) \left( \frac{d}{ds} \boldsymbol{\phi}_j(s) \right) \quad (24)$$

by using the definition for the time derivative

$$\lim_{\delta \rightarrow 0} \frac{\mathbf{g}(t + \delta + s) - \mathbf{g}(t + s)}{\delta} = \sum_{j=0}^{\infty} \lim_{\delta \rightarrow 0} \left[ \frac{w_j(\mathbf{x}(t + \delta)) - w_j(\mathbf{x}(t))}{\delta} \right] \boldsymbol{\phi}_j(s) = \sum_{j=0}^{\infty} w_j(\mathbf{x}(t)) \lim_{\delta \rightarrow 0} \left[ \frac{\boldsymbol{\phi}_j(s + \delta) - \boldsymbol{\phi}_j(s)}{\delta} \right] \quad (25)$$

**Theorem 1.** *Suppose  $g(t)$  and  $\{\boldsymbol{\phi}_j\}_{j=0}^{\infty}$  are  $\mathcal{C}^1$ . Suppose the series  $\sum_j w_j(\mathbf{x}(t)) \boldsymbol{\phi}'_j(s)$  and  $\sum_j w_j(\mathbf{x}(t)) \langle \boldsymbol{\phi}_j(s), \boldsymbol{\phi}_j(s) \rangle$  converge uniformly on  $[-\tau, \tau]$ . Then the action of the Koopman generator on these coordinates is given by*

$$\mathcal{K}w_j = \sum_{k=0}^{\infty} w_k K_{jk} \quad (26)$$

where

$$K_{jk} = \langle \boldsymbol{\phi}_j(s), \boldsymbol{\phi}'_k(s) \rangle = \int_{-\tau}^{\tau} \boldsymbol{\phi}_j(s)^T \boldsymbol{\phi}'_k(s) ds. \quad (27)$$

*Proof.* We begin by noting that

$$\mathbf{g}'(t + s) := \frac{\partial}{\partial t} \mathbf{g}(\mathbf{x}(t + s)) = \frac{\partial}{\partial s} \mathbf{g}(\mathbf{x}(t + s)) \quad (28)$$

Substituting equation (21) we obtain

$$\sum_{k=0}^{\infty} \boldsymbol{\phi}_k(s) \frac{d}{dt} w_k(\mathbf{x}(t)) = \sum_{k=0}^{\infty} \boldsymbol{\phi}'_k(s) w_k(\mathbf{x}(t)) \quad (29)$$

Multiplying both sides of this equation by  $\boldsymbol{\phi}_j(s)$ , integrating, and applying the orthonormality condition of this basis,  $\langle \boldsymbol{\phi}_j, \boldsymbol{\phi}_k \rangle = \delta_{jk}$ , we obtain

$$\begin{aligned} \sum_{k=0}^{\infty} \underbrace{\int_{-\tau}^{\tau} \boldsymbol{\phi}_j(s)^T \boldsymbol{\phi}_k(s) ds}_{=\delta_{jk}} \frac{d}{dt} w_k(\mathbf{x}(t)) &= \sum_{k=0}^{\infty} w_k(\mathbf{x}(t)) \int_{-\tau}^{\tau} \boldsymbol{\phi}_j(s)^T \boldsymbol{\phi}'_k(s) ds = \sum_{k=0}^{\infty} w_k(\mathbf{x}(t)) \langle \boldsymbol{\phi}_j(s), \boldsymbol{\phi}'_k(s) \rangle \\ \Rightarrow \frac{d}{dt} w_j(\mathbf{x}(t)) &= \sum_{k=0}^{\infty} w_k(\mathbf{x}(t)) \langle \boldsymbol{\phi}_j(s), \boldsymbol{\phi}'_k(s) \rangle = \sum_{k=0}^{\infty} w_k K_{jk} = \mathcal{K}w_j(\mathbf{x}(t)) \quad \forall j \end{aligned}$$

□

An analogous result holds for the discrete-time dynamics of the convolutional coordinates, with the additional assumption of analyticity and analytic continuability.

**Theorem 2.** *Let  $\mathbf{x}(t)$  be a differentiable function on  $\mathbb{R}$ . Suppose  $\mathbf{x}(t)$  is locally analytic everywhere with radius of convergence at least  $\tau + \Delta t$ . Let  $\{\phi_j\}_{j=0}^{\infty}$  be a differentiable, orthogonal basis of  $L^2[-\tau, \tau]$ . Suppose also that each  $\phi_j$  can be analytically continued to a radius  $\tau + \Delta t$ . Then the action of the Koopman operator  $\mathcal{K}_{\Delta t}$  on the convolutional coordinates  $w_j$  is given by*

$$\mathcal{K}_{\Delta t} w_j = \sum_k w_k \int_{-\tau}^{\tau} \phi_j(s) \phi_k(s + \Delta t) ds = \sum_k w_k \langle \phi_j(s), \phi_k(s + \Delta t) \rangle. \quad (30)$$

*Proof.* Let  $\hat{\phi}_k(t)$  denote the analytic continuation of  $\phi_k$  on the interval  $[-\tau - \Delta t, \tau + \Delta t]$ . We then have

$$\begin{aligned} \mathcal{K}_{\Delta t} w_j(\mathbf{x}(t)) &= w_j(\mathbf{x}(t + \Delta t)) \\ &= \int_{-\tau}^{\tau} \phi_j(s)^T \mathbf{g}(\mathbf{x}(t + \Delta t + s)) ds \\ &= \int_{-\tau}^{\tau} \phi_j(s) \sum_{k=0}^{\infty} w_k(\mathbf{x}(t)) \phi_k(s + \Delta t) ds \\ &= \sum_{k=0}^{\infty} w_k(\mathbf{x}(t)) \int_{-\tau}^{\tau} \phi_j(s)^T \phi_k(s + \Delta t) ds. \end{aligned}$$

□

In summary, the span of these convolutional coordinates  $\{w_j\}_{j=0}^{\infty}$  forms a Koopman-invariant subspace, and the action of the Koopman operator  $\mathcal{K}$  in this space can be naturally represented in component form as  $K_{ij}$ . While this *representation* is system-independent, the convolutional coordinates themselves are system-dependent.

## 4 SVD Convolutional Coordinates

In practice, we will not have access to an infinite set of smooth coordinates with which to embed our signal. We will generally be able to keep track of only a finite number of coordinates at any given time. Furthermore, we will usually not be working with ideal smooth trajectories, but instead with discretized trajectories limited by a finite sampling frequency. This latter condition puts a fundamental limit on the number of linearly independent coordinates that we can generate that are still *smooth* enough for finite difference approximations to effectively approximate the derivative of each coordinate basis vector. Since we can only consider a finite set of coordinates, it is imperative that we choose a set that effectively encodes the dynamics of our system. In general, an arbitrary basis will not be suitable. The reason for this is that the fixed linear relations are usually too rigid to effectively encode the dynamics without higher-order corrections. The spectrum of the estimated finite-dimensional linear system on the convolutional coordinates depends strictly on the choice of basis, and will generally not match that of the underlying system. This is a fundamental issue, particularly when the derived models have unstable eigenvalues.

To circumvent this issue, we need to pick a problem-specific basis. One option is to use the eigenfunctions of the autocorrelation function  $\mathbf{C}(t, s)$ , i.e. the functions  $\mathbf{u}_j(s)$  which satisfy the Fredholm integral equation of the second kind:

$$\int_{-\tau}^{\tau} \mathbf{C}(t, s) \mathbf{u}_j(s) ds = \lambda_j \mathbf{u}_j(t). \quad (31)$$

These vectors are equivalently the left singular vectors obtained from applying the SVD to the Hankel matrix  $\mathbf{H}$  of the trajectory. The trajectory can then be represented as

$$\mathbf{x}(t + s) = \sum_{j=0}^{\infty} \sigma_j \mathbf{u}_j(s) v_j(t) \quad (32)$$

where  $\{\mathbf{u}_j\}_{j=0}^\infty$  and  $\{v_j\}_{j=0}^\infty$  are orthonormal and  $\sigma_1 \geq \sigma_2 \geq \dots \geq 0$ .

Brunton et. al. [8] first used these coordinates as Koopman observables for a DMD algorithm, although they did not frame their results as such. They found that by using the singular vectors as a basis for the convolutional coordinates, they were able to obtain a subspace that was nearly Koopman invariant. However, their results were primarily empirical, without providing any theoretical guarantees on accuracy. Arbabi and Mezić [1] later studied some properties of these coordinates, but did not apply them to DMD directly.

Motivated by these results, we study these coordinates theoretically before outlining how these are estimated from data. We show that they have many interesting properties, including the following:

1. The predicted convolutional coordinate coefficients  $\langle \mathbf{u}_j, \mathbf{u}'_k \rangle$  for this basis match the output of the EDMD algorithm applied to the convolutional coordinates.
2. These coordinates are optimal for a system with  $r$  distinct Koopman eigenvalues in the sense that the first  $r$  convolutional coordinates provide a Koopman-invariant subspace that spans the first  $r$  Koopman eigenfunctions.

These properties motivate the application of these coordinates to dynamical systems, which is demonstrated in Sec. 5.

## 4.1 Spectral Dynamics in Delay Coordinates: Continuous and Discrete Formulation

The basis functions  $\{\mathbf{u}_j(s)\}_{j=0}^\infty$  are an *optimal* basis for representing the delay embedding  $\mathbf{x}(t+s)$  in the sense that the first  $r$  coordinates provide the closest subspace to the full space of coordinates. This basis also has a number of other attractive properties from a dynamical systems perspective. In particular, truncating the infinite-dimensional linear dynamics of the system (26) provides the best least-squares approximation to the true dynamics of the system. This result, which is directly related to the SVD of  $\mathbf{H} = \mathbf{U}\Sigma\mathbf{V}^*$ , is proven below:

**Theorem 3.** *Let  $\mathbf{v}(t) := [v_1, v_2, \dots, v_r]^T$  be the vector consisting of the first  $r$  coordinates  $v_j(t)$  and  $\mathbf{v}'(t) := \frac{d}{dt}\mathbf{v}(t)$ . Then the coefficients of the linear map  $\mathbf{T}$  advancing the  $\mathbf{v}(t)$ , i.e.  $\mathbf{v}'(t) = \mathbf{T}\mathbf{v}(t)$ , minimizing the RMS error*

$$E_{RMS} = \frac{1}{T} \sqrt{\int_0^T \|\mathbf{T}\mathbf{v}(t) - \mathbf{v}'(t)\|_2^2 dt}, \quad (33)$$

where the  $l_2$  norm is defined by  $\|\mathbf{v}\|_2 := \sqrt{\mathbf{v}^T \mathbf{v}}$ , are given by

$$T_{jk} = \frac{\sigma_k}{\sigma_j} K_{jk}. \quad (34)$$

*Proof.* We can rewrite the equation defining  $\mathbf{T}$  as follows:

$$(\mathbf{v}')^*(t) = \mathbf{v}^* \mathbf{T}^* \quad (35)$$

The solution to the least-square problem for  $\mathbf{T}^*$  takes the form

$$\mathbf{T}^* = (\mathbf{V}\mathbf{V}^*)^{-1} \mathbf{V}\mathbf{V}'^* \quad (36)$$

where  $\mathbf{V}$  and  $\mathbf{V}'$  contain the time series of each coordinate  $v_j(t)$  and its time derivative  $v'_j(t)$ , respectively, as a row. Since  $\mathbf{V}$  is unitary, this reduces to

$$\mathbf{T}^* = \mathbf{V}\mathbf{V}'^*. \quad (37)$$

or alternatively

$$\mathbf{T} = \mathbf{V}'\mathbf{V}^* \quad (38)$$

In component form, this gives

$$T_{jk} = \int_0^T v'_j(t) v_k^*(t) dt. \quad (39)$$

We can expand  $v'_j$  using (26) and noting that  $w_j = \sigma_j v_j$ :

$$v'_j(t) = \sum_{l=0}^{\infty} K_{jl} \frac{\sigma_l}{\sigma_j} v_l(t). \quad (40)$$

Substituting this into (39) gives

$$\begin{aligned} T_{jk} &= \int_0^T v_k^*(t) \sum_{l=0}^{\infty} K_{jl} \frac{\sigma_l}{\sigma_j} v_l(t) dt \\ &= \sum_{l=0}^{\infty} \frac{\sigma_l}{\sigma_j} K_{jl} \underbrace{\int_0^T v_k^*(t) v_l(t) dt}_{\delta_{kl}} \\ &= \frac{\sigma_k}{\sigma_j} K_{jk} \end{aligned}$$

□

**Remark 1.** This result holds identically for the linear map minimizing  $\|\mathbf{T}\mathbf{v}(t) - \mathbf{v}(t + \Delta t)\|_2$ , with the discrete time evolution coefficients given in (30). This linear map coincides with the map estimated by DMD on the convolutional coordinates.

**Remark 2.** This result also shows that the closest linear approximation of the associated convolutional coordinates  $w_j = \sigma_j v_j$  or  $\mathbf{w} = \mathbf{\Sigma}\mathbf{v}$ , are given simply by  $\mathbf{K} \approx \mathbf{\Sigma}^{-1}\mathbf{T}\mathbf{\Sigma}$ .

Another useful property of the SVD convolutional coordinates is that the Koopman eigenfunctions and eigenvalues of systems that admit a finite Koopman mode decomposition can be exactly recovered from the projections of the dynamics onto a finite set of singular vectors. Suppose that  $\mathbf{x}(t)$  admits the decomposition

$$\mathbf{x}(t) = \sum_{j=0}^r \mathbf{a}_j e^{\lambda_j t} \quad (41)$$

where the set of eigenvalues  $\{\lambda_j\}_{j=0}^r$  is finite, i.e. has cardinality  $|\{\lambda_j\}_{j=0}^r| = r$ . The finiteness of the spectrum is not reasonable for most general nonlinear systems with discrete spectra; however in these cases, the coefficients  $\mathbf{a}_j$  will vanish as  $j \rightarrow \infty$ , so we can obtain arbitrarily good approximations of these systems with large but finite truncations of the Koopman mode decomposition. To obtain the time-delay embedding of the trajectory, we compute  $\mathbf{x}(t + s)$ :

$$\mathbf{x}(t + s) = \sum_{j=0}^r \mathbf{a}_j e^{\lambda_j t} e^{\lambda_j s}. \quad (42)$$

Thus, in the delay-embedded space, the dynamical evolution is given by  $\sum_{j=0}^r \mathbf{v}_j e^{\lambda_j t}$ , where  $\mathbf{v}_j = \mathbf{a}_j e^{\lambda_j s}$ . Thus the delay-embedded state lies in the span of  $\{e^{\lambda_j s}\}_{j=0}^r$ . This is a finite-dimensional subspace and thus these windows are also in span of the first  $|\{\lambda\}|$  singular vectors. Since the singular vectors and the exponential vectors are related by a finite change of basis, it follows the dynamics (and in particular the spectrum) of the system are encoded exactly in the map  $\mathbf{T}$  of these convolutional coordinates. Furthermore, if the eigendecomposition of  $\mathbf{T}$  is given by  $\mathbf{T} = \mathbf{P}\mathbf{\Lambda}\mathbf{P}^{-1}$ , then the functions

$$v_j(\mathbf{x}(t)) = (\mathbf{P}^{-1}\mathbf{w}(\mathbf{x}(t)))_j \quad (43)$$

are eigenfunctions of the Koopman operator with associated eigenvalue  $\lambda_j$ . These can also be rewritten as follows:

$$v_j(\mathbf{x}(t)) = \int_{-\tau}^{\tau} \left\langle \sum_{k=0}^{\infty} (\mathbf{P}^{-1})_{jk} \mathbf{u}_k(s), \mathbf{x}(t+s) \right\rangle ds. \quad (44)$$

The eigenfunctions of the Koopman operator can thus be interpreted as convolutional coordinates of an associated *eigenfilter* basis  $\sum_{k=0}^r (\mathbf{P}^{-1})_{jk} \mathbf{u}_k(s)$  with the system trajectory.

While this result is useful, we may also be interested in understanding the SVD coordinate approximations to the Koopman operator without restrictions to cases where the system has purely discrete spectra. The following theorem helps guide our understanding of the structure of the resultant approximations:

**Theorem 4.** *Let  $\mathbf{x}(t)$  be bounded. Suppose we have estimated  $\mathbf{u}_j$ ,  $\sigma_j$  and  $v_j$  from a time-delay embedded  $\mathbf{x}$  from time 0 to time  $T$ . Suppose in the limit as  $T \rightarrow \infty$  that  $\sigma_j \rightarrow \infty$  holds for all singular values. Then in the limit as  $T \rightarrow \infty$  the map given in (34) is antisymmetric.*

*Proof.* Consider the product  $v_j(t)v_k(t)$ . Differentiating this gives

$$\frac{d}{dt} v_j v_k = v'_j v_k + v'_k v_j.$$

Integrating both sides from 0 to  $T$  and substituting the coefficients (34), we are left with

$$v_j(T)v_k(T) - v_j(0)v_k(0) = T_{jk} + T_{kj}. \quad (45)$$

The coordinate  $v_j(t)$  is normalized over the interval  $[0, T]$ , and the normalization factor is given by  $\frac{1}{\sigma_j}$ . Thus the following bound holds:

$$|v_j(t)| = \left| \frac{\int_{-\tau}^{\tau} \langle \mathbf{u}_j(s), \mathbf{x}(t+s) \rangle ds}{\sigma_j} \right| \leq \frac{1}{\sigma_j} \|\mathbf{u}_j\| \|\mathbf{x}_t\|.$$

Since  $\|\mathbf{u}_j\|$  and  $\|\mathbf{x}_t\|$  are uniformly bounded for all time lengths  $T$ , it follows that  $|v_j| \rightarrow 0$  as  $T \rightarrow \infty$ . Therefore in the limit as  $T \rightarrow \infty$  we obtain

$$T_{jk} = -T_{kj}. \quad (46)$$

□

One disadvantage of using principal components is that their average magnitude will depend on the estimation length  $T$  due to the normalization condition. This is problematic because as  $T \rightarrow \infty$  these trajectories tend to zero magnitude. Instead, we will usually want to model the respective convolutional coordinates, which are the non-normalized principal components. The linear model estimated for this system is related to the linear model for the principal components by the change of basis relation  $\hat{\mathbf{T}} = \Sigma^{-1} \mathbf{T} \Sigma$ , or in component form  $\hat{T}_{jk} = K_{jk} = T_{jk} \frac{\sigma_j}{\sigma_k}$ . This transformed matrix will generally not be antisymmetric; however, the spectrum of  $\hat{\mathbf{T}}$  will be identical to the spectrum of  $\mathbf{T}$ , which converges to the imaginary axis in the limit as  $T \rightarrow \infty$ . This result indicates that SVD coordinates may be effective at approximating systems with Koopman operators with purely imaginary spectra.

These properties give us the following corollary, which may have useful implications for understanding the spectral quality of these approximations to the Koopman operator:

**Corollary 1.** *Let  $i\alpha_1, i\alpha_2, \dots, i\alpha_r$  with  $\alpha_i \leq \alpha_j$  if  $i < j$  be the DMD eigenvalues for the first  $r$  convolutional coordinates, and let  $i\beta_1, i\beta_2, \dots, i\beta_{r+1}$  with  $\beta_i \leq \beta_j$  if  $i \leq j$  be the DMD eigenvalues for the first  $r+1$  convolutional coordinates. It follows from Cauchy's interleaving theorem that*

$$\beta_i \leq \alpha_i \leq \beta_{i+1}. \quad (47)$$

## 4.2 A Conjecture on the Error of HAVOK Approximations to the Koopman Operator

From the result of theorem 3 we can write  $E_{RMS}$  for the for the convolutional coordinates as

$$\begin{aligned} E_{RMS} &= \frac{1}{T} \sqrt{\int_0^T \sum_{j=1}^N \left( \sum_{k>N} K_{jk} w_j(t) \right)^2 dt} \\ &= \frac{1}{T} \sqrt{\sum_{j=1}^N \sum_{k>N} \sum_{l>N} \sigma_k \sigma_l K_{jk} K_{jl} \int_0^T v_j(t) v_l(t) dt} \\ &= \frac{1}{T} \sqrt{\sum_{j=1}^N \sum_{k>N} \sigma_k^2 K_{jk}^2}. \end{aligned}$$

The rate of convergence of this error is related to the respective rates of increase and decay of  $K_{jk}^2$  and  $\sigma_k^2$ . It has been empirically observed that the singular values of many systems of interest decay exponentially with  $k$ . It has also been formally shown that the decay of the singular values is related to the smoothness of the function  $x(t+p)$ . We paraphrase theorem 7.1 from [47] which gives bounds on  $\sigma_j$  in terms of the derivatives of  $x(t+p)$ :

**Theorem 5.** *If, for some  $v \geq 1$ , the functions  $x_t(p)$  have a  $v$ th derivative of variation uniformly bounded with respect to  $v$ , or if the corresponding assumption holds with the roles of  $t$  and  $p$  interchanged, then the singular values and approximation errors satisfy  $\sigma_k = O(k^{-v})$ . If, for some  $\rho > 1$ , the functions  $x_t(p)$  can be extended in the complex  $t$ -plane to analytic functions in the Bernstein  $\rho$ -ellipse scaled to  $[-\tau, \tau]$  uniformly bounded with respect to  $p$ , then the singular values and approximation errors satisfy  $\sigma_k = O(\rho^{-k})$ .*

While this addresses the question of the decrease of the singular values, the question of the increase in  $K_{jk}^2 = \langle \mathbf{u}_j, \mathbf{u}'_k \rangle^2$  is not well studied. To our knowledge, no results currently exist on the smoothness of the functions  $\mathbf{u}_k$ , nor on how their derivatives  $\mathbf{u}'_k$  scale with  $k$ . However, our empirical results are promising. In section 4, we will show empirically that the coefficient  $K_{jk}$  appear to scale only polynomially with  $k$ . We conjecture that a polynomial bound exists on the derivatives of the singular components in terms of  $k$  and thus that a polynomial or exponential bound exists on the total error  $E_{RMS}$  in terms of  $k$ .

If proven, this result could have significant implications for Koopman theory. It has been shown that the projections of the Koopman operator onto generic  $D$ -dimensional subspaces of observables converges to the Koopman operator as  $D \rightarrow \infty$  [19]. However, for finite  $D$ , the quality of these approximations is highly dependent on the choice of subspace, and for a generic family of observables it may be quite difficult to obtain convergence without exceedingly high dimensional states. A bound of the form conjectured above would guarantee that these representations converge quickly to a known precision in convolutional SVD coordinates for any (sufficiently smooth) dynamical system. We do not know of any other family of observables for which a similar bound exists.

## 4.3 Computing SVD Convolutional Coordinates from Data

In applications, we generally do not have access to the full trajectory  $\mathbf{x}(t)$ , but instead discretely sampled signal  $\mathbf{x}_k := \mathbf{x}(t_k)$  sampled with timestep  $\Delta t = t_{k+1} - t_k$ . We employ the following numerical approximations to compute the quantities relevant to our theory and as demonstrated for the examples in Sec. 5:

1. We first construct the Hankel matrix (??) from a sampled trajectory of the considered dynamical system. The dimension of this matrix is  $DN \times M$ , where  $D$  is the number of observables,  $N$  is the delay embedding dimension and  $M$  is the number of snapshots. Then the SVD of this matrix is computed to obtain approximations of  $\mathbf{u}_j(s)$  of (??) and  $v_j(t)$ . In general, only the first few singular vectors  $\mathbf{u}_j(s)$  will be well-approximated by the singular vectors  $\mathbf{u}_j$ , due to the exponential decay of the singular values. Instead of computing a full or thin SVD of  $\mathbf{H}$ , we can instead compute a partial SVD of some

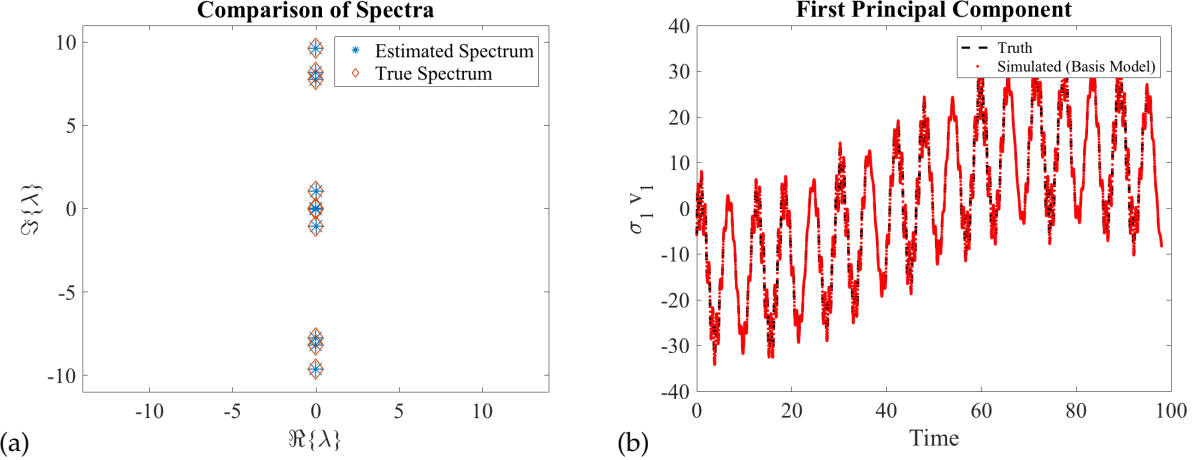


Figure 1: Delay embedding of a trajectory from a linear system with random imaginary eigenvalues: (a) reconstructed spectrum matches the true spectrum almost exactly, and (b) the true trajectory and reconstructed trajectory of the first convolutional coordinate fir with negligible error.

rank  $r \ll \min(N, M)$ . This approach is highly efficient without sacrificing any information about the dynamics. We also suggest an alternative approach for computing these observables and their dynamics by approximating the autocorrelation function, which is discussed in B.

2. We can compute the matrix elements  $K_{jk}$  either by computing  $\frac{\sigma_j}{\sigma_k} \langle \mathbf{v}_j, \mathbf{v}'_k \rangle$  or  $\langle \mathbf{u}_j, \mathbf{u}'_k \rangle$ . These approaches are of order  $O(r^2 M)$  and  $O(r^2 DN)$ , respectively, and can be used when the measurement states are are high- and low-dimensional, respectively. We compute the derivatives  $\mathbf{u}'_j$  and  $\mathbf{v}'_j$  using numerical finite differencing.
3. The dynamics of the convolutional coordinates are then approximated by

$$w_j(t) = \sum_{j=-\tau/\delta}^{\tau/\delta} \mathbf{u}_j \mathbf{y}_{t+k}. \quad (48)$$

## 5 Applications to Dynamical Systems

### 5.1 Linear Systems

The simplest possible setting for a Koopman analysis using a SVD delay embedding is a finite-dimensional linear system. As established previously, the dynamics of these systems are spectrally identical to the dynamics in a finite number of convolutional coordinates. Thus, linear systems are useful for illustrating the main principle of this method, as well as for highlighting some of the issues that arise when working with discrete signals instead of continuous functions. In particular, we consider a number of numerical experiments with real trajectories taken from linear systems with random imaginary spectra. A single coordinate is measured and then delay embedded. The SVD observables and associated linear models are computed using the algorithm in Sec. 4.3. We find that our method is able to exactly reconstruct these trajectories in almost all cases. A typical result is illustrated in Fig. 5.1.

A number of pathological cases exist for which our method does not perform as well as expected. The most fundamental case is that our method performs poorly if the frequencies in the dynamics are *close* with respect to  $\tau$ , i.e. when  $(\omega_j - \omega_k)\tau$  is small for a subset of frequencies so that the eigenvalues are nearly degenerate. While these eigenvalues would be closely matched in the linear model, the simulated trajectory using this model would often fail to match that of the original system. This can be explained as an effect of

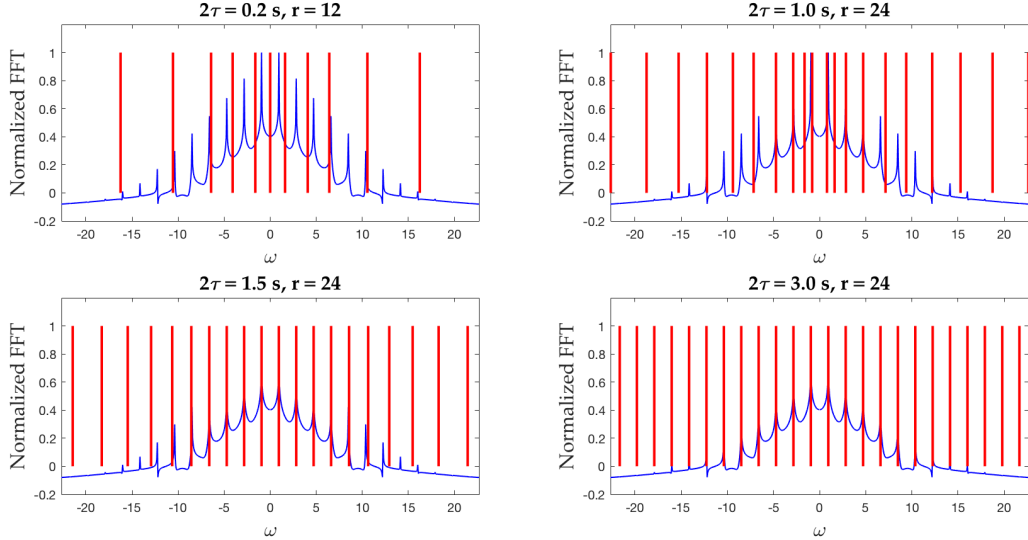


Figure 2: Comparison of the spectrum of the SVD coordinate operators on the Van der Pol attractor for  $\mu = 1$  and  $2\tau = 0.2, 1.0, 1.5$  and  $3.0$ . The Fourier transform of the trajectory is plotted in blue, and the locations of the imaginary component of the eigenvalues of the SVD coordinate operators are marked as red vertical lines. The spectrum of the operator matches the peaks in the Fourier spectrum for sufficiently large  $\tau$ . For smaller  $\tau$ , the spectrum appears distorted. This is likely related to the poor scaling properties of the eigenvectors discussed in section 5.1.

poor conditioning. Recall that the normalized eigenvectors associated with a frequency  $\omega$  are

$$v = \frac{1}{\sqrt{2\tau}} e^{i\omega t}.$$

The inner product between  $v_j$  and  $v_k$  is then given by

$$\langle v_k, v_j \rangle = \frac{1}{2\tau} \int_{-\tau}^{\tau} e^{-i\omega_k t} e^{i\omega_j t} dt = \frac{1}{2\tau} \frac{e^{i(\omega_j - \omega_k)t}}{i(\omega_j - \omega_k)} \Big|_{-\tau}^{\tau} = \text{sinc}((\omega_j - \omega_k)\tau).$$

As  $(\omega_j - \omega_k)\tau \rightarrow 0$  this term goes to 1, indicating that the eigenspaces converge. In this regime, the linear system is ill-conditioned, and small errors in the estimation of the eigenvectors can propagate catastrophically. Then, it may be necessary to avoid estimating the model directly from the SVD basis in order to obtain a more precise estimate. More generally, if the  $r$  eigenvectors occupy a smaller and smaller volume of state space, then the variance of their distribution becomes smaller and the singular values decay rapidly. This spectral crowding, i.e. many closely spaced eigenvalues, makes it difficult to resolve the dynamics of the system when the eigenvectors are close together. In such a regime, for improved robustness, we recommend computing DMD model from the full trajectories of the convolutional coordinates  $w_j$ , rather than the basis vectors  $u_j$ .

## 5.2 The Van der Pol Oscillator

The van der Pol system is a nonlinear second-order differential equation:

$$\frac{d^2x}{dt^2} - \mu(1 - x^2) \frac{dx}{dt} + x = 0. \quad (49)$$

In the small- $\mu$  limit, the van der Pol system reduces to a harmonic oscillator. For positive  $\mu$ , a trajectory starting off the attractor decays asymptotically onto a limit cycle in the phase space spanned by  $x$  and

$\dot{x} := \frac{d}{dt}x$ . Since the limit cycle is periodic, we expect the spectrum of the Koopman operator on the attractor to be discrete integer multiples of the fundamental frequency  $\omega$ . Since the spectrum is also discrete, we expect that the SVD delay embedding method should be able to exactly reconstruct these frequencies.

Importantly, nonlinearity in dynamical systems manifests two critical phenomenon: (i) the production of harmonic frequencies, and (ii) shifts in the underlying frequencies as a function of the strength of the nonlinearity. As will be shown by our time-delay embedding, the SVD coordinate system accurately extracts these manifestations. For the van der Pol system, a classical asymptotic expansion in the weakly nonlinear limit using a Poincaré-Lindstedt expansion [3, 16] with a *stretched* time coordinate is given by

$$\tau = \omega(\epsilon)t = (\omega_0 + \epsilon\omega_1 + \dots)t, \quad (50a)$$

$$x = x_0 + \epsilon x_1 + \epsilon^2 x_2 + \dots, \quad (50b)$$

where  $\epsilon = \mu \ll 1$ . The Fredholm-Alternative theorem allows us to determine the asymptotic corrections to the leading order sinusoidal oscillations so that

$$x(t) \approx 2 \cos \left[ (1 + 7\epsilon^2/16)t \right] + \epsilon \left[ \frac{3}{4} \sin \left[ (1 + 7\epsilon^2/16)t \right] - \frac{1}{4} \sin \left[ 3(1 + 7\epsilon^2/16)t \right] \right] + O(\epsilon^2). \quad (51)$$

Such asymptotic expansions not only allows one to compute the frequency shifts imposed by the nonlinearity, i.e. from  $\omega = 1$  to  $\omega = (1 + 7\epsilon^2/16)$ , but it also reveals the production of harmonics (the Koopman spectrum), as illustrated by the  $\sin[3\omega(\epsilon)t]$  term at  $O(\epsilon)$  which is generated by the cubic nonlinearity. At  $O(\epsilon^2)$ , the nonlinearity generates a  $\sin[5\omega(\epsilon)t]$  contribution and further corrections to the frequency. Although asymptotic expansions are insightful, they are only valid in the weakly nonlinear regime. The Koopman embedding proposed here can accurately compute the frequency shifts and harmonics (spectrum) generated from the nonlinearity even in the strongly nonlinear regime, allowing for improved analytic insight into nonlinear dynamical systems.

The van der Pol oscillator is simulated on the attractor for 100 time units with a time step of  $\Delta t = 0.001$ . We examine parameters  $\mu = 0.1, 0.5, 1.0$  and  $3.0$ , which represent different regimes ranging from weakly to strongly nonlinear dynamics. In all of these cases, the eigenvalues of the SVD coordinate operators matched the dominant spectral peaks of the system, provided the delay embedding window  $2\tau$  was chosen to be large enough. However, for sufficiently small  $\tau$ , the estimated spectrum did not match the peaks in the Fourier spectrum. This is likely related to the pathological behaviors with spectral crowding identified in section 5.1. In particular, the stronger the nonlinearity  $\mu$ , the larger the window size needed to adequately represent the spectrum. This was likely due to two related phenomena: The peaks of the higher-order frequencies increase as the nonlinearity increases, resulting in more *active* frequencies and thus more crowding. Furthermore, the fundamental frequency  $\omega$  decreases as  $\mu$  increases, exacerbating the spectral crowding issue. A topic of further study will be to relate the minimum window size  $2\tau$  to the magnitude of the nonlinearity.

Trajectories with initial conditions off of the attractor are analyzed. In this domain DMD-type linear models are not expected to perform well, since the spectrum of the Koopman operator is continuous in this regime, and thus no finite-dimensional linear model exists for these dynamics. The system is simulated with a randomly drawn initial condition off of the attractor and  $\mu = 1.0$ . For comparison, EDMD is applied to both a set of polynomial observables of order 6 and a set of SVD convolutional coordinates for varying window lengths. Instead of performing a delay-embedding with a single coordinate, we constructed the convolutional coordinates by delay embedding both the coordinates,  $x$  and  $\dot{x}$ . The reconstruction achieved using polynomial observables appears uniformly poor. Surprisingly, we found that by taking a similar number of SVD convolutional coordinates, we could reconstruct the trajectory exactly, despite the continuous spectrum. This result is illustrated in Fig. 3. The result is suggestive, but comes with the caveat that the window size necessary for such an accurate reconstruction is almost as long as the period of time it takes for the trajectory to decay onto the attractor. Nevertheless, this approach shows promise and may lead to future directions for approximating non-chaotic systems with continuous Koopman operator spectra.

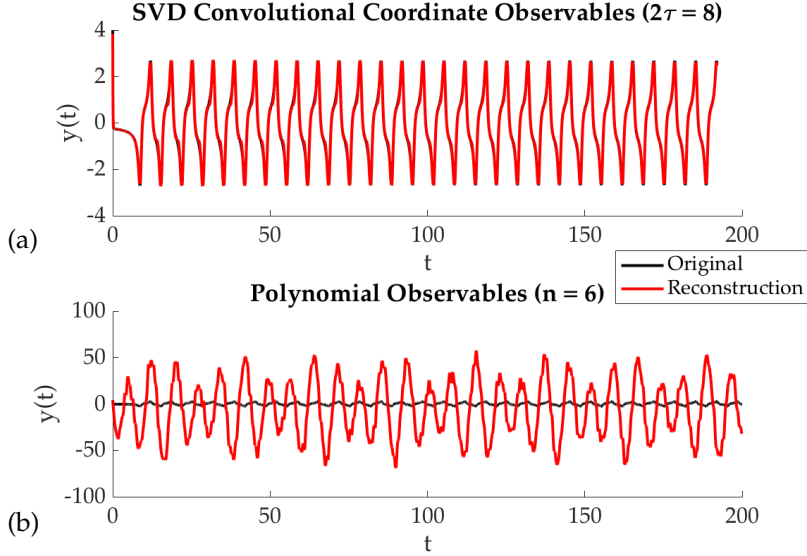


Figure 3: EDMD reconstruction of a trajectory from off the van der Pol attractor ( $\mu = 1.0$ ) with (a) 28 SVD Convolutional coordinate observables,  $2\tau = 8$ , and (b) using polynomial observables up to order 6 (28 terms).

### 5.3 Nonlinear Schrödinger Equation

In the previous examples, applications of SVD convolutional coordinates to dynamical systems of only low state dimension are considered. However, these methods can be applied to systems of arbitrary, possibly infinite dimension. As an example, we consider the nonlinear Schrödinger equation in one spatial direction:

$$iu_t + \frac{1}{2}u_{xx} + |u|^2u = 0. \quad (52)$$

This equation is nonlinear but admits soliton solutions that exhibit quasiperiodic behavior in time, and as such presents an interesting test case for Koopman spectral methods. Kutz et. al. [22] studied these solutions using several DMD-based algorithms. They found that kernel-DMD methods generally performed quite poorly for a wide variety of kernel functions. This result was surprising, given the simple structure present in the soliton solutions. This negative result shows the importance of choosing a good subspace of observables for accurate reconstruction. They found further that by augmenting the state with the nonlinear observable  $|u|^2u$ , which was motivated from the nonlinearity appearing in the original equation, they were able to achieve reconstruction with high accuracy outperforming all other choices of observables.

The nonlinear Schrödinger equation is simulated with the initial condition

$$u(x, 0) = 2\operatorname{sech}(x), \quad (53)$$

which is known to generate a soliton solution. The data is sampled across the spatial domain  $x \in [-15, 15]$ , over a time domain of  $t \in [0, 16\pi]$ , with 2000 time snapshots. The data is then split into a training set, on which the models are trained, and a test set, on which the models are validated by estimating the predictive accuracy of each method. Due to the poor performance of kernel-DMD on these solutions, we chose instead to benchmark our approach using conventional DMD and EDMD with the system-motivated observable  $|u|^2u$ . We computed the reconstruction error of each model for different choices of the truncation rank  $r$ .

Summarizing the results, the HAVOK method accurately extracts the quasiperiodic dynamics of the system. In contrast, the DMD with linear observables is able to capture qualitatively the overall periodicity but is not quantitatively accurate and suffered from poorer performance on the test set than on the training set. The HAVOK model achieves the lowest RMS error of any of the methods tested, which was achieved at

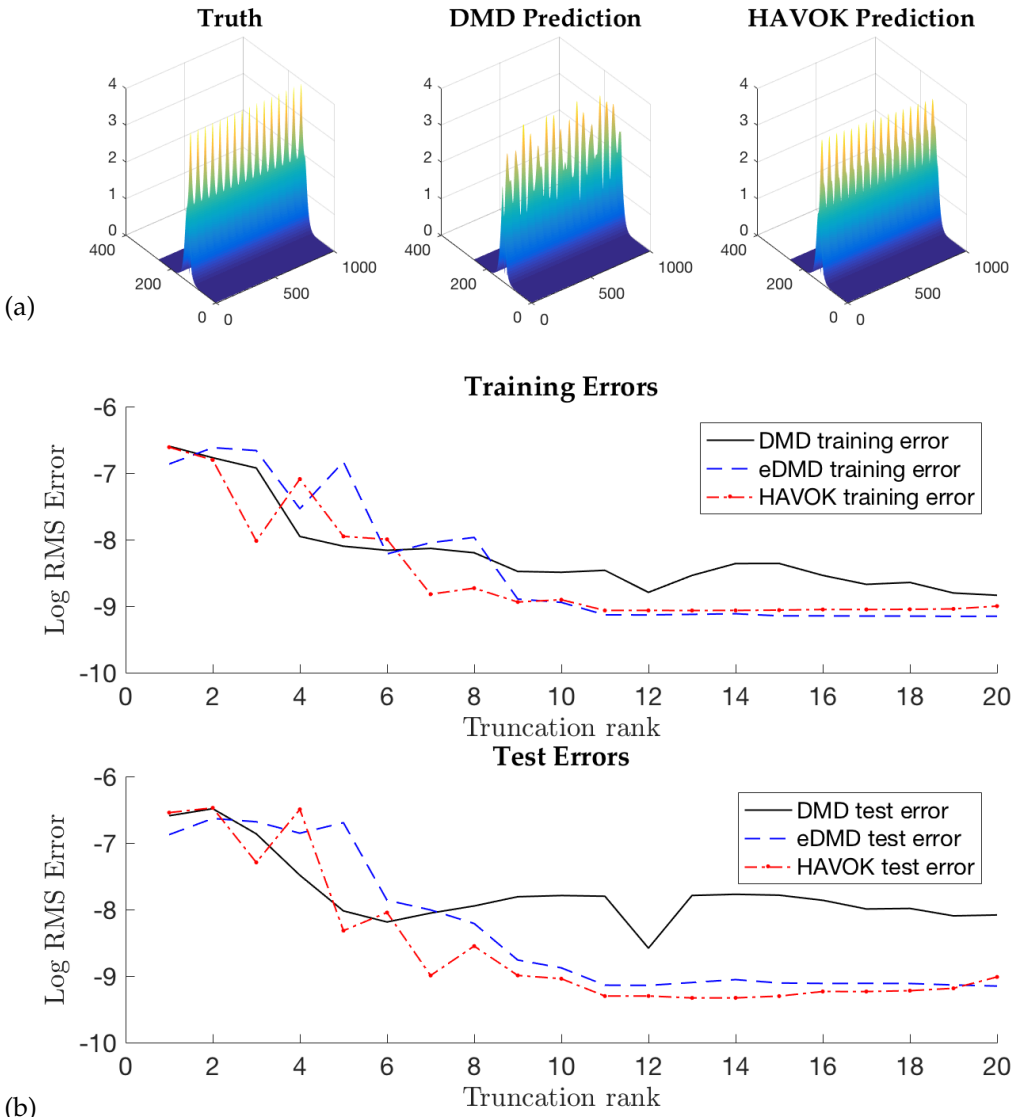


Figure 4: Prediction of the nonlinear Schrödinger equation: (a) True and predicted NLS solution using truncation rank  $r = 14$ . HAVOK achieves notably better reconstruction than DMD on linear observables. (b) Comparing the RMS prediction error of DMD, eDMD and HAVOK on the training and test data for increasing truncation rank. The SVD convolutional coordinate observables have similar training performance as eDMD with the physically motivated observable  $u|u|^2$ , and have the lowest test error of any of the methods (achieved at  $r = 14$ ). Interestingly, the HAVOK test error increases after  $r = 14$ , while the eDMD test error remains steady.

$r = 14$ . Interestingly, the HAVOK test error increases after  $r = 14$ , while the eDMD test error remains steady. Overall, the performance of the HAVOK method is generally comparable with the performance of eDMD with the physically motivated observable  $u|u|^2$ . The SVD convolutional coordinates are not chosen using a priori physical knowledge, so the fact that they achieved comparable or better performance is encouraging.

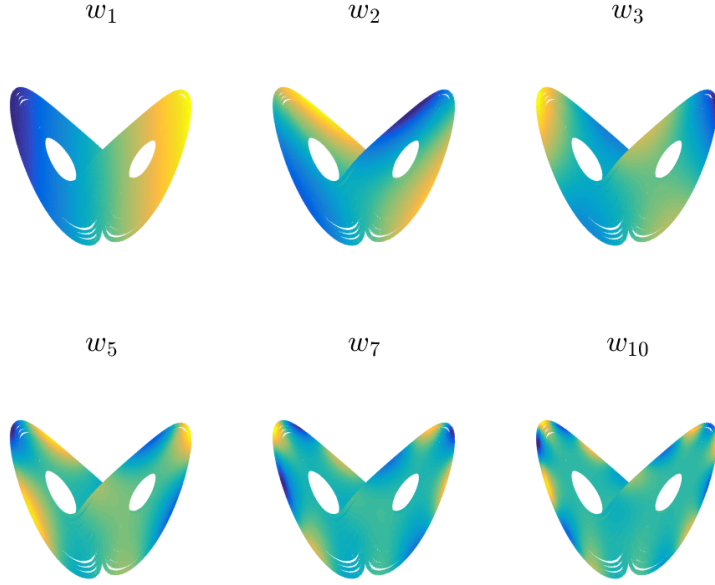


Figure 5: Convolutional coordinates  $w_1, w_2, w_3, w_5, w_7$ , and  $w_{10}$  visualized on the Lorenz attractor.

#### 5.4 Understanding Intermittent Forcing in the Lorenz System

It has been shown that chaotic systems do not admit exact finite-dimensional linear representations, as they possess mixed or purely continuous Koopman spectra [31]. In these cases, the Koopman operator may only have trivial (constant) eigenfunctions [18]. Nevertheless, there is interest in obtaining an approximate linearization that, while not globally accurate, captures some essential features of the dynamics.

Brunton et. al. studied this question in [8] using the methodology of time-delay embedding and principal components. They computed the Hankel principal components for a number of chaotic systems and estimated a linear system by applying DMD to these coordinates. While the resulting linear models were not closed and did not approximately represent the dynamics by themselves, they found that they were able to approximately close these models to very high accuracy by taking the highest-order convolutional coordinate as a random exogenous input to the model and simulating the other coordinates based on the derived linear dependencies. The authors of this paper were unable to explain the apparent success of this method theoretically. However, the results in this paper provide a natural justification for these results, as well as a number of other striking features of their models.

We first reproduce their results in the case of the Lorenz system. The Lorenz system

$$\dot{x}_1 = 10(x_2 - x_1) \quad (54a)$$

$$\dot{x}_2 = x_1(28 - x_3) - x_2 \quad (54b)$$

$$\dot{x}_3 = x_1x_2 - 8/3x_3 \quad (54c)$$

is sampled for 100 time units with a time step  $\Delta t = 0.001$ . A Hankel matrix is constructed from the sampled trajectory with delay dimension 100. The SVD of the Hankel matrix yields the  $\mathbf{U}$ ,  $\mathbf{S}$  and  $\mathbf{V}$  matrices. The trajectory in convolutional coordinates is then estimated as  $\mathbf{S}\mathbf{V}^\dagger$ . These results are plotted in figure 5.

Instead of applying DMD to the principal components, the model is derived analytically from the  $\mathbf{U}$  basis vectors. After normalization, this model matches the model derived in [8] with very high accuracy, both in the Frobenius norm and in the spectral norm. The structure of these models are illustrated in figure 6. The normalized SVD coordinate operator is nearly antisymmetric, as predicted by theorem 4. Interestingly, only the first off-diagonals are nearly nonzero, indicating that coefficients  $\frac{\sigma_k}{\sigma_j} \langle u_j, u'_k \rangle$  drop off quickly

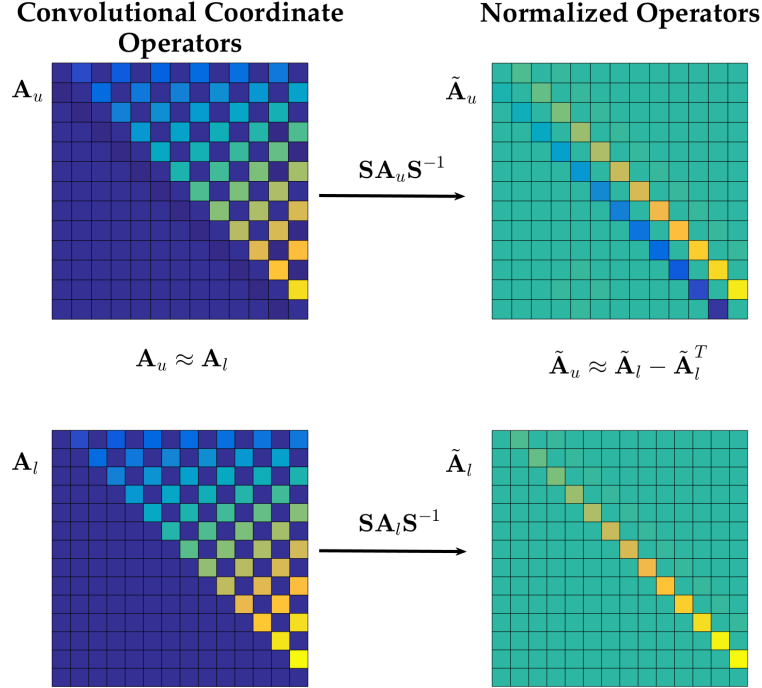


Figure 6: Relationship between operators for the Lorenz system: The linear model  $\mathbf{A}_u$  is estimated in the SVD coordinates. The normalized linear model is given by  $\tilde{\mathbf{A}}_u = \mathbf{S}^{-1} \mathbf{A}_u \mathbf{S}$ . The SVD-coordinate model is similar to the predicted linear model  $\mathbf{A}_l$  in Legendre coordinates. In contrast, the normalized model  $\tilde{\mathbf{A}}_l = \mathbf{S}^{-1} \mathbf{A}_l \mathbf{S}$  differs from  $\tilde{\mathbf{A}}_u$ , revealing how these operators encode very different dynamics. The coefficients of these operators appear to grow linearly in  $i$  and  $j$ . This connection explains the structure of the models derived in [8].

with  $j > k$ . This fact is related to the relative growth rates of the singular values and the coefficients  $\mathcal{A}_{jk}$ . As conjectured previously, the decay rate of  $\sigma_j$  is much stronger than the growth of  $\mathcal{A}_{jk}$ . This particular structure means that the derivative  $\dot{v}_j$  can be well-approximated by  $\mathbf{A}_{j(j-1)} v_{j-1} + \mathbf{A}_{j(j+1)} v_{j+1}$ . This dependency explains the *forcing* behavior observed in [8], in which the dynamics of the first  $r$  coordinates could be modeled by a linear model on the first  $r$  coordinates plus a linear forcing vector depending on the  $r+1$  coordinate.

It is instructive to compare the SVD coordinate model with the model predicted for Legendre convolutional coordinates, which are very close to the SVD coordinates [13]. The model for the Legendre coordinates is computed using the formulae derived in Appendix A. Prior to normalization, the SVD coordinate and Legendre coordinate operators appear nearly identical, although the SVD coordinate one has a small negative lower-triangular component. After normalization, however, the matrices appear very different. The Legendre coordinate model matches the upper triangular component of the SVD model, but has no corresponding subdiagonal component. This results in a highly unstable model. The negative subdiagonal component of the SVD model stabilizes the model and gives it an imaginary spectrum.

## 6 Summary and Discussion

In this paper, we studied the properties of *convolutional coordinates* on dynamical systems, constructed by convolving a basis of filters with the trajectories of the dynamical systems. We show that these coordinates naturally linearize system dynamics. For a given choice of basis used to construct the convolutional coordinates, the representation of the Koopman operator in these coordinates is shown to be system inde-

pendent. We derive these representations in terms of the basis functions and their derivatives. We consider the question of obtaining a good choice of basis for finite-dimensional approximations to the Koopman operator in convolutional coordinates. The eigenvectors of the autocorrelation function, or equivalently the singular vectors of the Hankel matrix, have several properties that make them attractive for this purpose, including that the analytically derived linear relations between these coordinates matches the approximations produced by applying DMD to these coordinates. We observe that these coordinates are also optimally parsimonious for finite discrete spectrum systems, and conjecture that restrictive error bounds exist for broader classes of systems. We validated our theoretical observations on a number of test systems, and found that these coordinates can excellently reconstruct the dynamics of these systems. We elaborate on the structure of the HAVOK models introduced by Brunton et. al. in [8] by noticing a connection with the Legendre polynomials and SVD coordinates.

This work suggest many interesting directions for future research. While we have conjectured that SVD convolutional coordinates have good error bounds for a wide class of systems, more work is needed to fully characterize the quality of these approximations. Since these observables have a very precise structure and many restrictive properties, it is expected that this analysis will be more fruitful than past analyses of generic families of observable functions. Further study is also needed of the effects of various parameters on these approximations, including the embedding dimension and the state dimension. It is also expected that these observables will provide good quality Koopman approximations for a wide variety of systems, and we hope that these methods will be applied to the large range of dynamical systems where Koopman spectral information is desired. Because of the considerable promise of leveraging Koopman linear representations for the control of nonlinear systems [20, 15, 37], it will be interesting to combine the delay coordinate representations with control approaches.

## Acknowledgements

SLB and JNK acknowledge funding support from the Defense Advanced Research Projects Agency (DARPA-PA-18-01-FP-125). SLB and EK acknowledge funding support from the Army Research Office (ARO W911NF-17-1-0306). EK gratefully acknowledges support by the "Washington Research Foundation Fund for Innovation in Data-Intensive Discovery" and a Data Science Environments project award from the Gordon and Betty Moore Foundation (Award #2013-10-29) and the Alfred P. Sloan Foundation (Award #3835). JNK acknowledges support from the Air Force Office of Scientific Research (AFOSR) grant FA9550-17-1-0329.

## Appendix A Delay Embedded Dynamics in Fourier and Legendre Bases

We can derive the form of the coefficients  $\mathbf{A}_{jk}$  for some example bases. The simplest such basis is the Fourier basis  $\{e^{\pi i n t / \tau}\}$ . The coefficients in this basis have the form

$$\mathbf{A}_{jk} = \frac{\pi i k}{\tau} \int_{-\tau}^{\tau} e^{\pi i (k-j)p / \tau} dp = 2\pi i k \delta_{jk}.$$

We can also consider these coefficients for a basis of orthogonal polynomials over  $[-\tau, \tau]$ . The foundation of our construction will be the Legendre polynomials, which are given by

$$P_l(x) = \frac{1}{2^l} \sum_{k=0}^{\text{floor}(l/2)} (-1)^k \binom{l}{k} \binom{2l-2k}{l} x^{l-2k}. \quad (55)$$

The Legendre polynomials have some useful properties. In particular, they are alternately even or odd, and the  $n$ th Legendre polynomial is orthogonal to the first  $n-1$  monomials  $x^0, \dots, x^{n-1}$ .

Instead of working with these polynomials directly, we will work with a rescaled Legendre basis, that

is orthonormal on  $[-\tau, \tau]$ . We define these functions as

$$\begin{aligned}\phi_l(x) &= \frac{P_l(x/\tau)}{\sqrt{\tau}\|P_l\|} = \frac{P_l(x/\tau)}{\sqrt{\tau}} \sqrt{\frac{2l+1}{2}} \\ &= \frac{1}{2^l} \sqrt{\frac{2l+1}{2\tau}} \sum_{k=0}^{\text{floor}(l/2)} (-1)^k \binom{l}{k} \binom{2l-2k}{l} \frac{x^{l-2k}}{\tau^{l-2k}}.\end{aligned}$$

For convenience we will abbreviate this expansion as

$$\phi_l(x) = C_l \sum_{k=0}^{\text{floor}(l/2)} B_{lk} x^{l-2k}.$$

The derivatives of these functions are given by

$$\phi'_l(x) = C_l \sum_{k=0}^{\text{floor}((l-1)/2)} B_{lk} (l-2k) x^{l-2k-1}.$$

The coefficients are given by

$$\mathbf{A}_{jk} = \int_{-\tau}^{\tau} \phi_j(p) \left( C_k \sum_{n=0}^{\text{floor}((k-1)/2)} (k-2n) B_{kn} p^{k-2n-1} \right) dp.$$

Note that the monomial exponents  $k-2n-1$  reach at most  $k-1$ . Since  $\phi_j$  is orthogonal to the first  $j-1$  monomials, if  $j \geq k$ ,  $\mathbf{A}_{jk} = 0$ . For  $j < k$ , this simplifies to

$$\begin{aligned}\mathbf{A}_{jk} &= \int_{-\tau}^{\tau} \phi_j(p) \left( C_k \sum_{n=0}^{\text{floor}((j+1-k)/2)} (k-2n) B_{kn} p^{k-2n-1} \right) dp \\ &= C_k \sum_{n=0}^{\text{floor}((j+1-k)/2)} \left( (k-2n) B_{kn} \int_{-\tau}^{\tau} \phi_j(p) p^{k-2n-1} dp \right).\end{aligned}$$

The inner product between  $\phi_j(p)$  and  $p^{k-2n-1}$  is given by

$$\begin{aligned}\int_{-\tau}^{\tau} \phi_j(p) p^{k-2n-1} dp &= \int_{-\tau}^{\tau} C_j \sum_{m=0}^{\text{floor}(j/2)} B_{jm} p^{(j+k)-2(m+n)-1} dp \\ &= C_j \sum_{m=0}^{\text{floor}(j/2)} \frac{B_{jm}}{(j+k)-2(m+n)-1} p^{(j+k)-2(m+n)} \Big|_{-\tau}^{\tau}.\end{aligned}$$

Evaluating this gives

$$\int_{-\tau}^{\tau} \phi_j(p) p^{k-2n-1} dp = \begin{cases} 2C_j \sum_{m=0}^{\text{floor}(j/2)} \frac{B_{jm}}{(j+k)-2(m+n)-1} \tau^{(j+k)-2(m+n)} & (j+k) \text{ odd} \\ 0 & (j+k) \text{ even.} \end{cases}$$

These can be substituted into our expression for  $\mathbf{A}_{jk}$  to obtain the full Legendre coordinates.

## Appendix B Fast Computation of Singular Vector Observables from the Autocorrelation Function

The naive approach to computing these observables from data requires computing the SVD of an  $N \times m$  Hankel matrix, where  $m$  is the number of snapshots and  $N$  is the length of the delay embedding. The cost

of this computation is  $O(N^2m + m^2N + \min(N^3, m^3))$ . In order to get effective approximations to smooth coordinates, we often need to take  $N$  large. At first glance, it may seem like the apparent advantage of having a parsimonious basis of observables is mitigated by this large up front computational cost.

To avoid this, we begin with the insight that we do not need to compute the full SVD, since we are only interested in computing the basis functions  $\mathbf{U}$ . These can be obtained by diagonalizing the autocovariance matrix:

$$\mathbf{A} = \mathbf{H}\mathbf{H}^T = \mathbf{U}\mathbf{S}^2\mathbf{U}^\dagger. \quad (56)$$

Naively this procedure requires  $N^2$  inner products of length- $m$  vectors to multiply to the two Hankel matrices. However, we can reduce this by using an analytic approximation of the autocovariance function. The autocovariance matrix is a discrete sampling of the autocovariance function, which is given by

$$A(p, q) = \lim_{T \rightarrow \infty} \frac{1}{2T} \int_{-T}^T x(t+p)x(t+q) dt = \overline{x(t+p)x(t+q)}. \quad (57)$$

The autocovariance is translationally invariant, i.e.  $A(p, q) = A(p+t, q+t)$ . We can therefore rewrite the autocorrelation as follows:

$$A(p, q) = \overline{x(t)x(t+(p-q))}. \quad (58)$$

We can expand this in  $(p-q)$  using a Taylor series approximation:

$$A(p, q) = \lim_{T \rightarrow \infty} \frac{1}{2T} \int_{-T}^T x(t) \sum_{n=0}^{\infty} \frac{x^{(n)}(t)(p-q)^n}{n!} dt \quad (59a)$$

$$= \sum_{n=0}^{\infty} \frac{(p-q)^n}{n!} \overline{x(t)x^{(n)}(t)}. \quad (59b)$$

If we truncate this Taylor series at some value  $n = n_{max}$ , we only need to compute  $n_{max}$  inner products of length  $m$  instead of  $N^2$ . This represents a significant cost savings over the naive SVD

This approach generalizes when the signal  $\mathbf{x}$  is multivariate. In this case, the autocorrelation is a tensor function:

$$\mathbf{A}(p, q) = \overline{\mathbf{x}(t+p)\mathbf{x}^*(t+q)}. \quad (60)$$

We can obtain a similar Taylor expansion for each component of the autocorrelation separately:

$$A_{jk}(p, q) = \sum_{n=0}^{\infty} \frac{(p-q)^n}{n!} \overline{x_j(t)x_k^{(n)}(t)}. \quad (61)$$

For a state with dimension  $k$ , the number of inner products in this approach is  $k^2 n_{max}$  as opposed to a naive  $k^2 N^2$ .

## References

- [1] Hassan Arbabi and Igor Mezic. Ergodic theory, dynamic mode decomposition, and computation of spectral properties of the Koopman operator. *SIAM Journal on Applied Dynamical Systems*, 16(4):2096–2126, 2017.
- [2] Travis Askham and J Nathan Kutz. Variable projection methods for an optimized dynamic mode decomposition. *SIAM Journal on Applied Dynamical Systems*, 17(1):380–416, 2018.
- [3] Carl M Bender and Steven A Orszag. *Advanced mathematical methods for scientists and engineers I: Asymptotic methods and perturbation theory*. Springer Science & Business Media, 2013.
- [4] D.S. Broomhead and Gregory P. King. Extracting qualitative dynamics from experimental data. *Physica D*, 20:217–236, 1986.

[5] Bingni W. Brunton, Lise A. Johnson, Jeffrey G. Ojemann, and J. Nathan Kutz. Extracting spatial-temporal coherent patterns in large-scale neural recordings using dynamic mode decomposition. *Journal of Neuroscience Methods*, 258:1–15, 2016.

[6] S. L. Brunton, B. W. Brunton, J. L. Proctor, and J. N Kutz. Koopman invariant subspaces and finite linear representations of nonlinear dynamical systems for control. *PLoS ONE*, 11(2):e0150171, 2016.

[7] S. L. Brunton, J. L. Proctor, and J. N. Kutz. Discovering governing equations from data by sparse identification of nonlinear dynamical systems. *Proceedings of the National Academy of Sciences*, 113(15):3932–3937, 2016.

[8] Steven L. Brunton, Bingni W. Brunton, Joshua L. Proctor, Eurika Kaiser, and J. Nathan Kutz. Chaos as an intermittently forced linear system. *Nature Communications*, 8, 2017.

[9] Marko Budišić, Ryan Mohr, and Igor Mezić. Applied Koopmanism a). *Chaos: An Interdisciplinary Journal of Nonlinear Science*, 22(4):047510, 2012.

[10] Suddhasattwa Das and Dimitrios Giannakis. Delay-coordinate maps and the spectra of Koopman operators. *arXiv preprint arXiv:1706.08544*, 2017.

[11] Matan Gavish and David L Donoho. The optimal hard threshold for singular values is  $4/\sqrt{3}$ . *IEEE Transactions on Information Theory*, 60(8):5040–5053, 2014.

[12] Dimitrios Giannakis and Andrew J Majda. Nonlinear Laplacian spectral analysis for time series with intermittency and low-frequency variability. *Proceedings of the National Academy of Sciences*, 109(7):2222–2227, 2012.

[13] Martin Casdagli Stephen Eubank John F. Gibson, J. Doyne Farmer. An analytic approach to practical state space reconstruction. *Physica D*, 57:1–30, 1992.

[14] Jer-Nan Juang and Richard S. Pappa. *Journal of Guidance, Control, and Dynamics*, (5):620–627.

[15] E. Kaiser, J. N. Kutz, and S. L. Brunton. Data-driven discovery of Koopman eigenfunctions for control. *arXiv preprint arXiv:1707.01146*, 2017.

[16] Jirayr Kevorkian and Julian D Cole. *Perturbation methods in applied mathematics*, volume 34. Springer Science & Business Media, 2013.

[17] B.O. Koopman. Hamiltonian systems and transformation in hilbert space. *Proceedings of the National Academy of Sciences of the United States of America*, 17(5):315–318, 1931.

[18] B.O. Koopman and J. von Neumann. Dynamical systems of continuous spectra. *Proceedings of the National Academy of Sciences of the United States of America*, 18(3):255–263, 1932.

[19] Milan Korda and Igor Mezić. On convergence of extended dynamic mode decomposition to the Koopman operator. *Journal of Nonlinear Science*, 28:687–710, 2017.

[20] Milan Korda and Igor Mezić. Linear predictors for nonlinear dynamical systems: Koopman operator meets model predictive control. *Automatica*, 93:149–160, 2018.

[21] J. N. Kutz, S. L. Brunton, B. W. Brunton, and J. L. Proctor. *Dynamic Mode Decomposition: Data-Driven Modeling of Complex Systems*. SIAM, 2016.

[22] J. Nathan Kutz, Joshua L. Proctor, and Steven L. Brunton. Koopman theory for partial differential equations. *Arxiv Preprint*, 2016.

[23] Yueheng Lan and Igor Mezić. Linearization in the large of nonlinear systems and Koopman operator spectrum. *Physica D: Nonlinear Phenomena*, 242(1):42–53, 2013.

[24] Andrzej Lasota and Michael C. Mackey. *Chaos, Fractals, and Noise: Stochastic Aspects of Dynamics*, volume 97 of *Applied Mathematical Sciences*. Springer-Verlag, New York, 2 edition, 1994.

[25] Soledad Le Clainche and José M. Vega. Higher order dynamic mode decomposition. *SIAM Journal on Applied Dynamical Systems*, 16(2):882–925, 2017.

[26] Qianxiao Li, Felix Dietrich, Erik M. Boltt, and Ioannis G. Kevrekidis. Extended dynamic mode decomposition with dictionary learning: a data-driven adaptive spectral decomposition of the Koopman operator. *Chaos: An Interdisciplinary Journal of Nonlinear Science*, 27, 2017.

[27] W. Liebert and H.G. Schuster. Proper choice of the time delay for the analysis of chaotic time series. *Physics Letters A*, 142:107–111, 1988.

[28] Bethany Lusch, J Nathan Kutz, and Steven L Brunton. Deep learning for universal linear embeddings of nonlinear dynamics. *arXiv preprint arXiv:1712.09707*, 2017.

[29] Andreas Mardt, Luca Pasquali, Hao Wu, and Frank Noé. VAMPnets: Deep learning of molecular kinetics. *Nature Communications*, 9(5), 2018.

[30] I. Mezić. *Spectral operator methods in dynamical systems: Theory and applications*. Springer, 2018.

[31] Igor Mezić. Spectral properties of dynamical systems, model reduction and decompositions. 2002.

[32] Igor Mezić. Spectral properties of dynamical systems, model reduction and decompositions. *Nonlinear Dynamics*, 41(1-3):309–325, 2005.

[33] Igor Mezic. Koopman operator spectrum and data analysis. *arXiv preprint arXiv:1702.07597*, 2017.

[34] Frank Noé and Feliks Nüske. A variational approach to modeling slow processes in stochastic dynamical systems. *Multiscale Modeling & Simulation*, 11(2):635–655, 2013.

[35] Feliks Nüske, Bettina G Keller, Guillermo Pérez-Hernández, Antonia SJS Mey, and Frank Noé. Variational approach to molecular kinetics. *Journal of chemical theory and computation*, 10(4):1739–1752, 2014.

[36] Samuel E Otto and Clarence W Rowley. Linearly-recurrent autoencoder networks for learning dynamics. *arXiv preprint arXiv:1712.01378*, 2017.

[37] Sebastian Peitz and Stefan Klus. Koopman operator-based model reduction for switched-system control of pdes. *arXiv preprint arXiv:1710.06759*, 2017.

[38] Clarence W. Rowley, Igor Mezic, Shervin Bagheri, Philipp Schlatter, and Dan S. Henningson. Spectral analysis of nonlinear flows. *Journal of Fluid Mechanics*, 641:115–127, 2009.

[39] P. J. Schmid. Dynamic mode decomposition of numerical and experimental data. *Journal of Fluid Mechanics*, 656:5–28, August 2010.

[40] P. J. Schmid and J. Sesterhenn. Dynamic mode decomposition of numerical and experimental data. In *61st Annual Meeting of the APS Division of Fluid Dynamics*. American Physical Society, November 2008.

[41] Peter J. Schmid. Dynamic mode decomposition of numerical and experimental data. *Journal of Fluid Mechanics*, 656:5–28, 2007.

[42] Yoshihiko Susuki and Igor Mezić. A prony approximation of Koopman mode decomposition. In *Decision and Control (CDC), 2015 IEEE 54th Annual Conference on*, pages 7022–7027. IEEE, 2015.

[43] Naoya Takeishi, Yoshinobu Kawahara, Yasuo Tabei, and Takehisa Yairi. Bayesian dynamic mode decomposition. *Twenty-Sixth International Joint Conference on Artificial Intelligence*, 2017.

[44] Naoya Takeishi, Yoshinobu Kawahara, and Takehisa Yairi. *Physical Review E*, page 033310.

[45] Naoya Takeishi, Yoshinobu Kawahara, and Takehisa Yairi. Learning Koopman invariant subspaces for dynamic mode decomposition. In *Advances in Neural Information Processing Systems*, pages 1130–1140, 2017.

- [46] Floris Takens. Detecting strange attractors in turbulence. *Dynamical Systems and Turbulence, Lecture Notes in Mathematics*, 1981.
- [47] A. Townsend and L.N. Trefethen. Continuous analogues of matrix factorizations. *Proceedings of the Royal Society A*, 471, 2015.
- [48] J. H. Tu, C. W. Rowley, D. M. Luchtenburg, S. L. Brunton, and J. N. Kutz. On dynamic mode decomposition: theory and applications. *Journal of Computational Dynamics*, 1(2):391–421, 2014.
- [49] R. Vautard and M. Ghil. Singular spectrum analysis in nonlinear dynamics, with applications to paleoclimatic time series. *Physica D*, 35:395–424, 1989.
- [50] Christoph Wehmeyer and Frank Noé. Time-lagged autoencoders: Deep learning of slow collective variables for molecular kinetics. *arXiv preprint arXiv:1710.11239*, 2017.
- [51] Matthew O. Williams, Ioannis G. Kevrekidis, and Clarence W. Rowley. A data-driven approximation of the Koopman operator: Extending dynamic mode decomposition. *Journal of Nonlinear Science*, 25:1307–1346, 2015.
- [52] Enoch Yeung, Soumya Kundu, and Nathan Hudas. Learning deep neural network representations for Koopman operators of nonlinear dynamical systems. *arXiv preprint arXiv:1708.06850*, 2017.